

การกักเก็บสารเชิงซ้อนแบบอินคลูชันของ 5,7-ไดเมทอกซีฟลาโวน/ไฮดรอกซีโพรพิล
ไซโคลเดกซ์ทรินในอนุภาคไลโปซอม

นายศุภชัย ทรงงาม

วิทยานิพนธ์นี้เป็นส่วนหนึ่งของการศึกษาตามหลักสูตรปริญญาวิทยาศาสตรมหาบัณฑิต
สาขาวิชาปิโตรเคมีและวิทยาศาสตร์พอลิเมอร์
คณะวิทยาศาสตร์ จุฬาลงกรณ์มหาวิทยาลัย
ปีการศึกษา 2554

ลิขสิทธิ์ของจุฬาลงกรณ์มหาวิทยาลัย
บทคัดย่อและแฟ้มข้อมูลฉบับเต็มของวิทยานิพนธ์ตั้งแต่ปีการศึกษา 2554 ที่ให้บริการในคลังปัญญาจุฬาฯ (CUIR)
เป็นแฟ้มข้อมูลของนิสิตเจ้าของวิทยานิพนธ์ที่ส่งผ่านทางบัณฑิตวิทยาลัย

The abstract and full text of theses from the academic year 2011 in Chulalongkorn University Intellectual Repository (CUIR)
are the thesis authors' files submitted through the Graduate School.

ENCAPSULATION OF 5,7-DIMETHOXYFLAVONE/
HYDROXYPROPYLCYCLODEXTRIN INCLUSION COMPLEXES IN
CHITOSAN PARTICLES

Mr. Supachai Songngam

A Thesis Submitted in Partial Fulfillment of the Requirements
for the Degree of Master of Science Program in Petrochemistry and Polymer Science

Faculty of Science

Chulalongkorn University

Academic Year 2011

Copyright of Chulalongkorn University

Thesis Title ENCAPSULATION OF 5,7-DIMETHOXYFLAVONE/
HYDROXYPROPYLCYCLODEXTRIN INCLUSION
COMPLEXES IN CHITOSAN PARTICLES

By Mr. Supachai Songngam

Field of Study Petrochemistry and Polymer Science

Thesis Advisor Assistant Professor Pattara Sawasdee, Ph.D.

Thesis Co-advisor Krisana Siraleartmukul, Ph.D.

Accepted by the Faculty of Science, Chulalongkorn University in
Partial Fulfillment of the Requirements for the Master's Degree

.....Dean of the Faculty of Science
(Professor Supot Hannongbua, Dr.rer.nat.)

THESIS COMMITTEE

..... Chairman
(Associate Professor Supawan Tantayanon, Ph.D.)

..... Thesis Advisor
(Assistant Professor Pattara Sawasdee, Ph.D.)

..... Thesis Co-advisor
(Krisana Siraleartmukul, Ph.D.)

..... Examiner
(Assistant Professor Varawut Tangpasuthadol, Ph.D.)

..... External Examiner
(Assistant Professor Boon-ek Yingyongnarongkul, Ph.D.)

ศุภชัย ทรงงาม: การกักเก็บสารเชิงซ้อนแบบอินคลูชันของ 5,7-ไดเมทอกซีฟลาโวน/
ไฮดรอกซีโพรพิลไซโคลเดกซ์ทรินในอนุภาคไคโตซาน (ENCAPSULATION OF 5,7-
DIMETHOXYFLAVONE/HYDROXYPROPYLCYCLODEXTRIN INCLUSION
COMPLEXES IN CHITOSAN PARTICLES) อ. ที่ปรึกษาวิทยานิพนธ์หลัก:
ผศ. ดร.พัฒนรา สวัสดิ์, อ. ที่ปรึกษาวิทยานิพนธ์ร่วม: อ. ดร.กฤษณา ศิริเลิศมุกด, 80 หน้า.

สาร 5,7-ไดเมทอกซีฟลาโวน คือ สารในกลุ่มฟลาโวนอยด์ ที่มีฤทธิ์ทางเภสัชวิทยาที่น่าสนใจ แต่เนื่องจากสารนี้ละลายในน้ำได้ค่อนข้างต่ำ การนำไปพัฒนาเป็นยาหรืออาหารเสริมเพื่อสุขภาพจึงทำได้ยาก ดังนั้นงานวิจัยนี้จึงมุ่งเน้นศึกษาการปรับปรุงคุณสมบัติไม่ชอบน้ำของสารออกฤทธิ์ดังกล่าวเพื่อให้สามารถละลายน้ำได้ดี โดยใช้วิธีทำให้เกิดสารประกอบเชิงซ้อนระหว่างสาร 5,7-ไดเมทอกซีฟลาโวนกับ 2-ไฮดรอกซีโพรพิลเบต้าไซโคลเดกซ์ทรินด้วยวิธีทำให้แห้งแบบเย็นเยือกแข็ง จากการศึกษาวัฏภาคการละลาย พบว่า สารประกอบเชิงซ้อนที่เกิดขึ้นมีค่าคงที่ความคงตัวเท่ากับ 1840 โมลาร์⁻¹ อัตราส่วนการเกิดสารประกอบเชิงซ้อนเกิดแบบ 1:1 อัตราส่วนโมลาร์ และได้ตรวจวิเคราะห์ยืนยันสารประกอบเชิงซ้อนที่เกิดขึ้นโดยวิธีฟูเรียร์ทรานฟอร์มอินฟราเรดสเปกโทรสโกปี ดิสเพอเรนเชียลสแกนนิ่งแคลอริเมตรี เอกซ์เรย์ดิฟแฟรกโทเมตรี และวิธีโปรตอนนิวเคลียร์แมกเนติกเรโซแนนซ์สเปกโทรสโกปี นอกจากนี้ ยังได้กักเก็บสารประกอบเชิงซ้อนที่เตรียมได้ในอนุภาคนาโนไคโตซาน โดยเตรียมอนุภาคนาโนไคโตซานด้วยเทคนิคการเกิดเจลระหว่างประจุของสารร่วมกับเทคนิคอัลตราโซนิเคชัน โดยเทคนิคอัลตราโซนิเคชันสามารถช่วยลดขนาดอนุภาคและช่วยเพิ่มประสิทธิภาพในการกักเก็บสารประกอบเชิงซ้อน การอัลตราโซนิเคชันอนุภาคไคโตซานที่กักเก็บสารประกอบเชิงซ้อนที่อัตราส่วน 4/2/1 โดยน้ำหนักของ ไคโตซาน/สารประกอบเชิงซ้อน/ไตรโพลีฟอสเฟต เป็นเวลา 5 นาที พบว่าให้ประสิทธิภาพการกักเก็บสารประกอบเชิงซ้อนสูงมากกว่า 60 เปอร์เซ็นต์ ด้วยขนาดอนุภาค 203 ± 3 นาโนเมตร และจากการศึกษาประสิทธิภาพการปลดปล่อยสารประกอบเชิงซ้อนจากอนุภาคนาโนไคโตซานที่ pH 1.2 และ pH 7.4 พบว่าอนุภาคนาโนไคโตซานมีการควบคุมการปลดปล่อยสารประกอบเชิงซ้อนอย่างรวดเร็วในช่วงต้นหลังจากนั้นจึงค่อยๆปลดปล่อยช้าลง ซึ่งสามารถปลดปล่อยสารประกอบเชิงซ้อนได้มากถึง 74 เปอร์เซ็นต์และ 62.8 เปอร์เซ็นต์ภายใน 24 ชั่วโมง ตามลำดับ

สาขาวิชา ปิโตรเคมีและวิทยาศาสตร์พอลิเมอร์ ลายมือชื่อนิสิต.....
ปีการศึกษา.....2554..... ลายมือชื่อ อ. ที่ปรึกษาวิทยานิพนธ์หลัก.....
ลายมือชื่อ อ. ที่ปรึกษาวิทยานิพนธ์ร่วม.....

5272569223 : MAJOR PETROCHEMISTRY AND POLYMER SCIENCE

KEYWORDS : 5,7-DIMETHOXYFLAVONE/ 2-HYDROXYPROPYL- β -
CYCLODEXTRIN/ INCLUSION COMPLEX/ CHITOSAN/ IONOTROPIC
GELATION/ NANOPARTICLES

SUPACHAI SONGNGAM: ENCAPSULATION OF 5,7-DIMETHOXYFLAVONE/HYDROXYPROPYLCYCLODEXTRIN INCLUSION COMPLEXES IN CHITOSAN PARTICLES. ADVISOR: ASST. PROF. PATTARA SAWASDEE, Ph.D., CO-ADVISOR: KRISANA SIRALEARTMUKUL, Ph.D., 80 pp.

5,7-Dimethoxyflavone (5,7-DMF) is a flavonoid reported to have many pharmacological properties. However, the pharmaceutical uses of this compound were limited due to its low water solubility. In this research, the water solubility of 5,7-DMF was improved by inclusion complex with 2-hydroxypropyl- β -cyclodextrin (HP β CD) using a lyophilizing method. Phase solubility showed stability constant of 1840 M^{-1} while Job's method affirmed 1:1 stoichiometry. Furthermore, FTIR, DSC, XRD, 1D, and 2D NMR were performed to prove the formation of inclusion complex. Moreover, the 5,7-DMF/HP β CD inclusion complexes were further loaded in chitosan nanoparticles. The loaded chitosan nanoparticles were prepared using ionotropic gelation and ultrasonication method. The ultrasonication could be used for decreasing the particle size and increasing the entrapment efficiency. Treated ultrasonication for 5 minute, chitosan nanoparticles containing 5,7-DMF/HP β CD inclusion complex (IC-uCSNP) with the ratio of chitosan/inclusion complex/TPP as 4/2/1 w/w/w have a high entrapment efficiency (> 60%) with average size of $203 \pm 3 \text{ nm}$. Controlled release studies performed *in vitro* at pH 1.2 and pH 7.4 showed an initial burst effect and followed by a slow 5,7-DMF/HP β CD inclusion complex release (74% and 62.8% within 24 h, respectively).

Field of Study: Petrochemistry and Polymer Science Student's Signature.....

Academic Year:2011..... Advisor's Signature.....

Co-advisor's Signature.....

ACKNOWLEDGEMENTS

The author would like to express my deep gratitude to my advisor, Assistant Professor Dr. Pattara Sawasdee, and Dr. Krisana Siraleartmukul (the Center of Chitin-Chitosan Biomaterial, Metallurgy and Materials Science Research Institute of Chulalongkorn University) for guidance, supervision and helpful suggestion throughout the course of this research.

The author also would like to thank to Associate Professor Dr. Supawan Tantayanon, Assistant Professor Dr. Varawut Tangpasuthadol and Assistant Professor Dr. Boon-ek Yingyongnarongkul (Faculty of Science, Ramkhamhaeng University), for serving as chairman and member of thesis committee whose comment have been especially valuable.

Definitely, this research cannot be completed without kindness and helpful of many people. The author also thanks the Center of Chitin-Chitosan Biomaterial, Metallurgy and Materials Science Research Institute of Chulalongkorn University for providing the equipment, chemicals, and facilities. I thank the Higher Education Research Promotion and National Research University Project of Thailand, Office of the Higher Education Commission FW645A and the National Center of Excellence for Petroleum, Petrochemicals, and Advanced Materials (NCE-PPAM), Graduate School from Chulalongkorn University, for financial support. I thank National Nanotechnology Center (NANOTEC) for facilitating the Zetasizer Nano ZS for a particle size measurement.

I sincerely thank Department of Chemistry, Chulalongkorn University and Scientific and Technological Research Equipment Center, Chulalongkorn University. In addition, I also thank members of Natural Products Research Unit for their encouragement and generous helps. Furthermore, many thanks are going to generous help of my friends and whose suggestion and support are throughout this research. Finally, I own deep gratitude to my family, especially my father and mother for their love and encouragement.

CONTENTS

	Page
ABTRACTS IN THAI.....	iv
ABSTRACTS IN ENGLISH.....	v
ACKNOWLEDGEMENTS.....	vi
CONTENTS.....	vii
LIST OF TABLES.....	x
LIST OF FIGURES.....	xii
LIST OF ABBREVIATIONS.....	xv
CHAPTER I INTRODUCTION.....	1
1.1 Introduction.....	1
1.2 The objectives of research.....	3
1.3 The scope of research.....	3
CHAPTER II THEORY AND LITERATURE REVIEWS.....	5
2.1 5,7-Dimethoxyflavone from <i>Kaempferia parviflora</i>	5
2.2 Cyclodextrins.....	7
2.2.1 Structure and physicochemical properties.....	7
2.2.2 Inclusion complex formation.....	10
2.2.3 Phase solubility analysis.....	11
2.2.4 Inclusion complex of flavonoids and other active compounds with cyclodextrins.....	13
2.3 Encapsulation by chitosan.....	17
2.3.1 Encapsulation.....	18
2.3.2 Chitosan and inclusion complex.....	19
2.3.3 Ionic gelation and ultrasonication method.....	22
2.3.4 Controlled release behavior of drug from chitosan particles.....	24
CHAPTER III EXPERIMENTAL.....	27
3.1 Chemicals and materials	27

	Page
3.2 Instruments.....	28
3.3 Method.....	29
PART I: Improvement the water solubility of 5,7-DMF.....	29
3.3.1 Preparation inclusion complexes of 5,7-DMF with different cyclodextrins.....	29
3.3.2 Phase solubility studies.....	29
3.3.3 Stoichiometry determination.....	29
3.3.4 Preparation 5,7-DMF/HP β CD inclusion complex.....	30
3.3.5 Characterization of 5,7-DMF/HP β CD inclusion complex.....	30
3.3.5.1 Fourier-Transform infrared spectroscopy.....	30
3.3.5.2 Differential scanning calorimetry analysis.....	31
3.3.5.3 X-ray diffractometry analysis.....	31
3.3.5.4 NMR spectroscopy.....	31
PART II: Encapsulation 5,7-DMF/HP β CD inclusion complex in chitosan nanoparticle	31
3.3.6 Preparation chitosan nanoparticles for characterization morphology.....	31
3.3.7 Preparation 5,7-DMF/HP β CD loaded chitosan nanoparticles for characterization morphology.....	32
3.3.8 Preparation 5,7-DMF/HP β CD loaded chitosan nanoparticles for <i>in vitro</i> release studies.....	32
3.3.9 Characterization of nanoparticles.....	32
3.3.10 Entrapment efficiency and loading capacity.....	33
3.3.11 <i>In vitro</i> release studies.....	34
3.3.12 Statistical analysis.....	35
CHAPTER IV RESULTS AND DISCUSSION.....	36
PART I: Improvement the water solubility of 5,7-DMF.....	36

	Page
4.1 Preliminary studies.....	36
4.2 Inclusion complex of 5,7-DMF with HP β CD.....	37
4.2.1 Phase solubility studies.....	37
4.2.2 Stoichiometry determination.....	39
4.2.3 Characterization of 5,7-DMF/HP β CD inclusion complex.....	40
4.2.3.1 Fourier-transform infrared spectroscopy.....	40
4.2.3.2 Differential scanning calorimetry analysis.....	43
4.2.3.3 X-ray diffractometry analysis.....	43
4.2.3.4 NMR spectroscopy.....	46
PART II: Encapsulation 5,7-DMF/HP β CD inclusion complex in chitosan nanoparticle	49
4.3 Preparation of chitosan nanoparticles.....	49
4.4 Preparation of 5,7-DMF/HP β CD loaded chitosan nanoparticles.....	53
4.5 <i>In vitro</i> release studies.....	56
CHAPTER V CONCLUSION.....	59
REFERENCES.....	60
APPENDICES.....	66
Appendix A.....	67
Appendix B.....	71
Appendix C.....	74
Appendix D.....	75
Appendix E.....	76
Appendix F.....	78
VITAE.....	80

LIST OF TABLES

		Page
Table 2.1	Some physicochemical properties of cyclodextrins.....	9
Table 3.1	Instruments.....	28
Table 4.1	Solubility of 5,7-DMF in 0-10 mM HP β CD concentration at 25 °C.....	38
Table 4.2	Wavenumbers (cm ⁻¹) and assignments for the bands observed in FTIR spectra of 5,7-DMF, HP β CD and inclusion complex.....	41
Table 4.3	The chemical shifts (δ) of HP β CD and 5,7-DMF/HP β CD inclusion complex in D ₂ O.....	46
Table 4.4	Physicochemical properties of chitosan particles following ultrasonication at specified duration time.....	50
Table 4.5	Physicochemical properties of IC-CSNP treated by ultrasonication in the difference concentrations of 5,7-DMF/HP β CD inclusion complexes.....	54
Table 4.6	Entrapment efficiency (%EE) and loading capacity (%LC) of IC-uCSNP.....	55
Table A1	The absorbance of 5,7-DMF in the presence of HP β CD (before extraction) in 25 ml of deionized water and the absorbance of 5,7-DMF in the absence of HP β CD (after extraction) in 25 ml of ethanol.....	69
Table A2	The absorbance of 5,7-DMF in the presence of HP β CD in the 25 ml of the difference solvents.....	70
Table B1	The absorbance of 5,7-DMF in ethanol solution determined at 264 nm.....	72
Table C1	The Solubility data of 5,7-DMF in various HP β CD concentrations.....	74
Table D1	Absorbances of 5,7-DMF/HP β CD, 5,7-DMF pure and Δ Absorbance in deionized water.....	75

	Page
Table F1 Percentage of inclusion complex release from chitosan nanoparticles at pH 1.2.....	78
Table F2 Percentage of inclusion complex release from chitosan nanoparticles at pH 7.4.....	79

LIST OF FIGURES

	Page
Figure 1.1 Chemical structure of 5,7-DMF.....	1
Figure 1.2 Chemical structure of HP β CD.....	2
Figure 1.3 Chemical structure of chitosan.....	3
Figure 2.1 The rhizomes of <i>Kaempferia parviflora</i>	5
Figure 2.2 Structures of isolated flavones from the rhizomes of <i>K. parviflora</i>	7
Figure 2.3 Chemical structures of α -, β -, and γ -cyclodextrins.....	8
Figure 2.4 Chemical structures and toroidal shape of β -cyclodextrins.....	8
Figure 2.5 Chemical structures of 2-Hydroxypropyl- β -cyclodextrin.....	9
Figure 2.6 Phase solubility of A-type and B-type diagram.....	11
Figure 2.7 A _L type of phase solubility of Artemether/HP β CD host-guest system.....	13
Figure 2.8 Possible inclusion mode and significant NOESY correlations of the crassicauline A/ β -cyclodextrin inclusion complex.....	15
Figure 2.9 Possible inclusion mode and significant NOESY correlations of the taxifolin/ β -cyclodextrin, taxifolin/HP β CD, taxifolin/ α -cyclodextrin, and taxifolin/ γ -cyclodextrin inclusion complexes.....	17
Figure 2.10 Different types of active compound micro or nanoparticles.....	18
Figure 2.11 Structure of chitin and chitosan.....	19
Figure 2.12 TEM images of chitosan nanoparticles with 25 mM of HP β CD.....	20
Figure 2.13 SEM image of methotrexate and calcium folinate loaded chitosan/ β -cyclodextrin nanoparticles.....	21
Figure 2.14 Chemical structure of chitosan ionically crosslinked with TPP.....	23

	Page
Figure 2.15 The plasma concentration of drug in the patient as a function of time after administration.....	25
Figure 2.16 Mechanism of drug release from particulate systems.....	26
Figure 4.1 UV spectra of 5,7-DMF (a) and 5,7-DMF in the presence of (b) HP β CD, (c) γ -CD, (d) β -CD, and (e) α -CD.....	37
Figure 4.2 Phase solubility diagram for the 5,7-DMF/HP β CD system.....	39
Figure 4.3 Continuous variation plot for the 5,7-DMF/HP β CD system from absorbance measurements.....	40
Figure 4.4 The FTIR spectra of (a) 5,7-DMF (b) HP β CD (c) inclusion complex and (d) physical mixture.....	42
Figure 4.5 The DSC thermograms of (a) 5,7-DMF (b) HP β CD (c) inclusion complex and (d) physical mixture.....	44
Figure 4.6 The XRD patterns of (a) 5,7-DMF (b) HP β CD (c) inclusion complex and (d) physical mixture.....	45
Figure 4.7 ¹ H NMR spectra of 5,7-DMF in CDCl ₃ and HP β CD in the absence and presence of 5,7-DMF.....	47
Figure 4.8 NOESY spectrum of 5,7-DMF/HP β CD inclusion complex.....	48
Figure 4.9 Possible inclusion mode of the 5,7-DMF/HP β CD complex.....	48
Figure 4.10 Size distribution graphs of chitosan nanoparticle.....	51
Figure 4.11 SEM images for chitosan nanoparticles.....	52
Figure 4.12 SEM images for IC-uCSNP.....	55
Figure 4.13 TEM images for IC-uCSNP.....	56
Figure 4.14 <i>In vitro</i> release profile of 5,7-DMF/HP β CD inclusion complex from chitosan nanoparticles at pH 1.2 and pH 7.4.....	58
Figure A1 UV spectra of (a) 5,7-DMF in the presence of HP β CD, (b) 5,7-DMF, (c) HP β CD.....	68
Figure B2 The standard calibration curve of 5,7-DMF in ethanol.....	73

	Page
Figure E1 The size distribution graph of IC-uCSNP at ratio of chitosan/inclusion complex/TPP as 4/2/1 (w/w/w).....	76
Figure E2 The size distribution graph of IC-uCSNP at ratio of chitosan/inclusion complex/TPP as 4/4/1 (w/w/w).....	76
Figure E3 The size distribution graph of IC-uCSNP at ratio of chitosan/inclusion complex/TPP as 4/8/1 (w/w/w).....	77

LIST OF ABBREVIATIONS

%	percentage
α	alpha
β	beta
ATR-IR	Attenuated Total Reflectance-Infrared
CD	cyclodextrin
CS	chitosan
CSNP	chitosan nanoparticle
CSNPs	chitosan nanoparticles
$^{\circ}\text{C}$	degree Celsius (centigrade)
DSC	Differential Scanning Calorimeter
5,7-DMF	5,7-dimethoxyflavone
%DD	degree of deacetylation
EE	entrapment efficiency
<i>et al.</i>	et alli, and other
FTIR	Fourier Transform Infrared Spectrophotometer
g	gram
γ	gamma
h	hour
HP β CD	hydroxypropyl-beta-cyclodextrin
ICCSNP	inclusion complexes loaded chitosan nanoparticles
IC-uCSNP	ultrasonicated inclusion complex loaded chitosan nanoparticle
LC	loading capacity
mg	milligram
mV	millivolt
min	minute
ml	milliliter
mM	millimolar

mmol	millimole
\overline{M}_w	molecular weight
nm	nanometer
NMR	nuclear magnetic resonance
PBS	phosphate buffer saline
PDI	polydispersity index
pH	power of hydrogen ion or the negative logarithm (base ten)
ppm	part per million
RT	room temperature
ref	reference
rpm	round per minute
SD	standard deviation
SEM	Scanning Electron Microscope
TEM	Transmission Electron Microscope
TPP	sodium tripolyphosphate
uCSNP	chitosan nanoparticle treated with ultrasonication
UV/Vis	ultraviolet/visible
v/v	volume by volume
λ	wavelength
w/v	weight by volume
w/w	weight by weight
XRD	X-ray diffractometer

CHAPTER I

INTRODUCTION

1.1 Introduction

Kaempferia parviflora Wall. Ex Baker (Zingiberaceae) or Kra-Chai-Dam is a health promoting herb in Thailand which have been commonly used for illness treatment such as gout, stomach discomfort, and gastrointestinal disorders [1]. The previous studies reported that the isolated flavonoids from the rhizomes of this plant exhibited a variety of biological activities such as anti-mycobacterial, anti-fungal, and anti-plasmodial activities [2]. Moreover, 5,7-dimethoxyflavone (5,7-DMF) (Figure 1.1), a major compound of *K. parviflora*, was reported to possess many pharmacological properties, for examples, anti-cholinestase, anti-phosphodiesterase type 5, anti-pyretic, anti-inflammatory, and cancer chemopreventive activities [3-6]. However, its use in pharmaceutical field was limited due to its low water solubility.

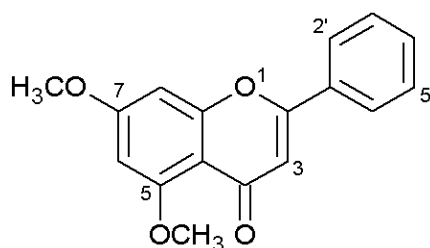


Figure 1.1 Chemical structure of 5,7-DMF

Cyclodextrins (CDs) are cyclic oligosaccharides which present a hydrophilic of outer surfaces and a central cavity is hydrophobic. CDs can encapsulate a variety of hydrophobic compounds to form inclusion complexes *via* host-guest interactions. The inclusion complexes with CDs have been successfully enhanced water solubility, bioavailability, and stability of many hydrophobic compounds in the pharmaceutical field [7].

2-Hydroxypropyl- β -cyclodextrins (HP β CDs) (Figure 1.2) is a water soluble derivative of β -CD which has high water solubility compared with α -CD, β -CD, and γ -CD. Moreover, HP β CDs are tolerated in human body with oral and intravenous administrations [8]. An inclusion complex of 5,7-DMF with HP β CD was prepared by lyophilization method and characterized its physicochemical properties by FTIR, DSC, XRD, 1D, and 2D NMR spectroscopic analysis.

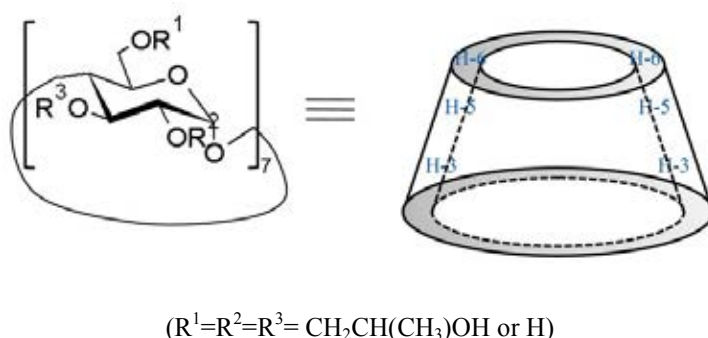


Figure 1.2 Chemical structure of HP β CD

In addition, the clinical uses of CDs have been restricted despite the fact that CDs have been successfully improved water solubility of poorly water soluble compounds due to its low absorbed from gastrointestinal tract for oral administration. However, the absorbability of CDs from gastrointestinal tract can be increased by its encapsulation in mucoadhesive nanocarriers not only to improve mucoadhesive properties but also to control drug release. Chitosan (Figure 1.3) is one of biodegradable polymers which have been commonly used for encapsulating drug and forming nanoparticle. Chitosan nanoparticles have a lot of advantage properties such as non-toxicity, biodegradability, biocompatibility, and mucoadhesion [9]. Moreover, there are some reports indicated that novel chitosan-cyclodextrin nanoparticles were able to entrap and improve the water solubility, bioavailability, and stability of hydrophobic drugs [10].

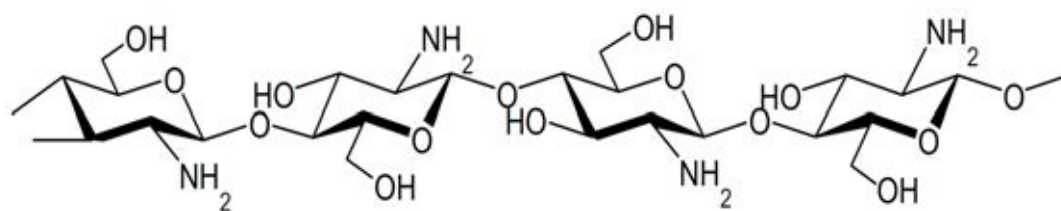


Figure 1.3 Chemical structure of chitosan

In this work, chitosan was used as a material to encapsulate an inclusion complex of 5,7-DMF with HP β CD. Moreover, to reduce size of encapsulated particle, ultrasonication was used to treat the 5,7-DMF/HP β CD inclusion complex loaded chitosan particles with the aim of nanoparticle size. The physicochemical properties of resulting nanoparticles were analyzed by particle size analyzer, SEM, and TEM. Moreover, entrapment efficiency, loading capacity, and *in vitro* release study were also evaluated.

1.2 The objectives of research

1.2.1 To enhance the water solubility of 5,7-DMF by inclusion complex with HP β CD

1.2.2 To prepare 5,7-DMF/HP β CD inclusion complex loaded in chitosan nanoparticle by ionotropic gelation and ultrasonication methods.

1.3 The scope of research

The research study was divided into two parts. The first part reported the improvement of the water solubility of 5,7-DMF by complexation with HP β CD using lyophilization method. The stoichiometry of host and guest were characterized by phase solubility and the continuous variation (Job's plot) method. In addition, the characteristics of the supramolecular structure of 5,7-DMF/HP β CD inclusion complex were investigated by FTIR, DSC, XRD, 1D, and 2D NMR spectroscopic analysis.

The second part reported the encapsulation of 5,7-DMF/HP β CD inclusion complex in chitosan nanoparticles by ionotropic gelation and ultrasonication methods. The resulting nanoparticles were characterized their morphology, size distribution, zeta potential, entrapment efficiency, loading capacity, and *in vitro* releasing.

CHAPTER II

THEORY AND LITERATURE REVIEWS

Most active compounds, isolated from herbal plants, have a variety of bioactivities but their low water solubility properties were a main problem for pharmaceutical uses. Therefore, water solubility improvement of these compounds is important together with enhance their control release behaviors and mucoadhesion by encapsulation with biopolymers are interesting.

2.1 5,7-Dimethoxyflavone from *Kaempferia parviflora*

Kaempferia parviflora Wall. Ex. Baker (local name: Kra-Chai-Dam, family: Zingiberaceae) is an herbal plant in Thailand (Figure 2.1). The rhizomes of this plant have been used in traditional medicines for health promoting and treatment of various diseases such as allergy, gastrointestinal disorders, and fungal infection impotence [11]. In Thailand, daily drink of the alcohol macerated rhizomes of *K. parviflora* is believed to have sexual enhancing activities or enhance erectile function.

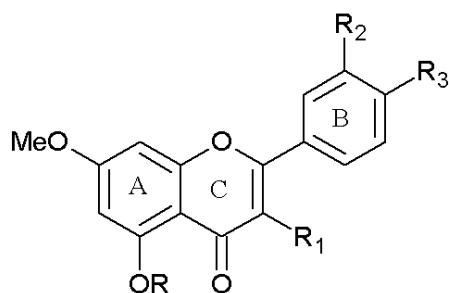
The compounds isolated from this plant have been reported to show a variety of biological activities such as anti-inflammatory [12], anti-allergic [13], vasorelaxation and anti-spasmodic [14], anti-gastric ulcer [15], anti-mycobacterial, anti-fungal, and anti-plasmodial activities [2] together with the promotion of nitric oxide production [16], and increasing testosterone levels [4].



Figure 2.1 The rhizomes of *Kaempferia parviflora*

The major compounds found in *K. parviflora* are flavonoids. Sawasdee *et al.* [3] reported the isolation of 13 flavonoids from the rhizomes of this plant. The chemical structures of these flavonoids were shown in Figure 2.2. Among of them, 5,7-dimethoxyflavone (5,7-DMF) is one of the active compounds (compound 7 in Figure 2.2). This compound was reported to possess a wide spectrum of pharmacological properties. It showed the potential chemopreventive effect to human cancer at liver, lung, mouth and esophagus [6]. Tep-areenan *et al.* [4] reported that 5,7-DMF has a vasodilator effect in the rat aorta which may be used as a medical plant for treatment of cardiovascular diseases. Sawasdee *et al.* [3] studied acetylcholinesterase (AChE) and butyrylcholinesterase (BChE) inhibitory activities of flavonoids isolated from *K. parviflora*. The results indicated that 5,7-DMF showed a high BChE selectivity with 85% inhibition activity at the concentration of 0.1 mg/ml. Tassanee *et al.* [5] reported the *in vivo* anti-inflammatory and anti-pyretic activities of 5,7-DMF. This compound exhibited anti-inflammatory effect in comparable with a standard anti-inflammatory drugs; prednisolone, hydrocortisone, indomethacin, and aspirin. Moreover, 5,7-DMF showed anti-pyretic activity greater than aspirin in the yeast-induced hyperthermia model.

According to a wide spectrum of pharmacological properties of 5,7-DMF, it is interesting to develop this compound as a drug. However, due to its low water solubility the extended tests of this compound in *in vivo* models and pharmaceutical uses are difficult.



- | | |
|----------------------------------------------------------------------|-------------------------------------------------------------------------|
| 1: R, R ₂ , R ₃ = H; R ₁ = OMe | 8: R = Me; R ₁ , R ₃ = OMe; R ₂ , = H |
| 2: R, R ₁ , R ₂ , R ₃ = H | 9: R = Me; R ₁ , R ₂ , R ₃ = OMe |
| 3: R, R ₂ = H; R ₃ = OMe | 10: R = Me; R ₁ = OMe; R ₂ , R ₃ = H |
| 4: R = H; R ₁ , R ₂ , R ₃ = OMe | 11: R = H; R ₁ , R ₃ = OMe; R ₂ , = OH |
| 5: R = Me; R ₁ = OMe; R ₂ , R ₃ = H | 12: R, R ₁ = H; R ₂ , R ₃ = OMe |
| 6: R = Me; R ₁ , R ₂ = H; R ₃ = OMe | 13: R, R ₁ , R ₂ = H; R ₃ = OH |
| 7: R = Me; R ₁ , R ₂ , R ₃ = H | |

Figure 2.2 Structures of isolated flavones from the rhizomes of *K. parviflora*.

2.2 Cyclodextrins

2.2.1 Structure and physicochemical properties

Cyclodextrins are non-toxic cyclic (α -1,4)-linked oligosaccharides of α -D-glucopyranose containing a relatively hydrophilic of outer surfaces and central cavity is hydrophobic. The most common cyclodextrins are of three types; α -, β -, γ -cyclodextrins consisting of six, seven, and eight α -(1,4)-linked glycosyl units, respectively (Figure 2.3) [17]. According to lack of free rotation about the bonds connecting the glucopyranose units, the shape of cyclodextrins is not regular

cylindrical but is cone or toroidal shaped (Figure 2.4). Based on this architecture, the primary hydroxyl groups are located on the narrow side and the secondary hydroxyl groups are located on the wide side. The non-polar C3-H group, C5-H group, and a ring of glucosidic oxygen are at inside of the cavity. This makes cyclodextrins exterior hydrophilic whereas the cavity is hydrophobic. Hence, cyclodextrins can encapsulate variety hydrophobic compounds to form inclusion complexes *via* host-guest interactions.

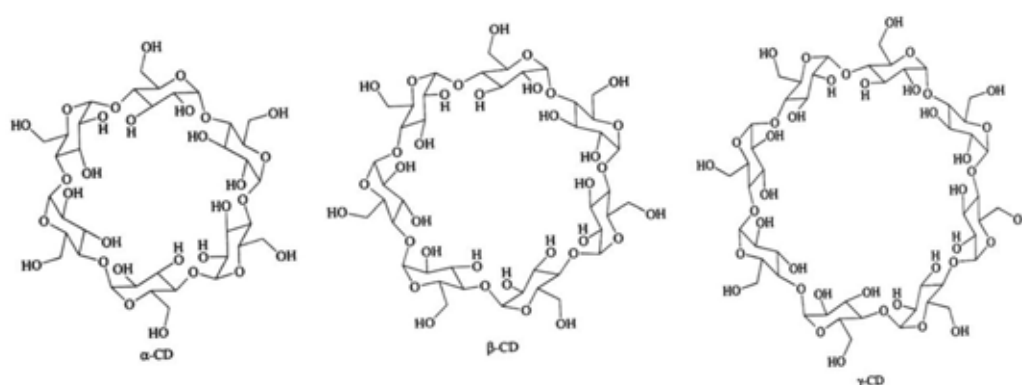


Figure 2.3 Chemical structures of α -, β - and γ -cyclodextrins. (Astray et al, 2009)

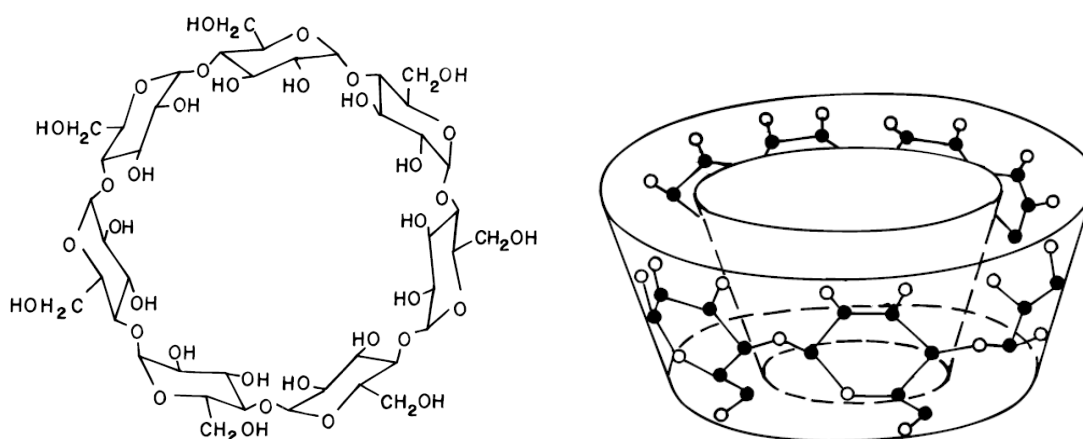


Figure 2.4 Chemical structures and toroidal shape of β -cyclodextrins. (Lofssan and Brewster, 1996)

The degree of substitution (DS) has important in the water solubility of cyclodextrin and its complexing ability. Therefore, an optimum level of the degree of substitution improves the water solubility of cyclodextrins but the capacity or efficiency of cyclodextrins complexing was impaired by the steric hindrances of cyclodextrin molecules. 2-Hydroxypropyl- β -cyclodextrin (HP β CD) (Figure 2.5) is a hydroxyalkyl derivative of β -cyclodextrin with a low degree of the degree of substitution (low surface activity) to show the good properties of complexing. Moreover, HP β CD has high water solubility compared with α -, β -, and γ -cyclodextrins.

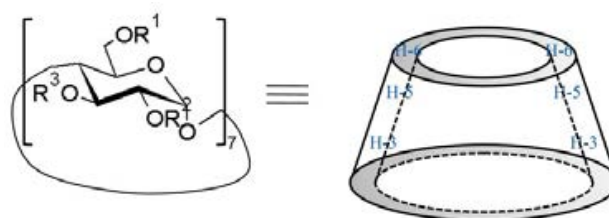


Figure 2.5 Chemical structures of 2-Hydroxypropyl- β -cyclodextrin (HP β CD).

The α -, β -, γ -cyclodextrins, and HP β CD have the melting points between 240-265 °C consistent with their stable crystal lattice structures [18]. The main physicochemical properties of cyclodextrins are given in Table 2.1.

Table 2.1 Some physicochemical properties of cyclodextrins [19]

	α -CD	β -CD	γ -CD	HP β CD
No. of glucopyranose units	6	7	8	7
Central cavity diameter (Å)	4.7-5.3	6.0-6.5	7.5-8.3	6.0-6.5
Molecular weight (g/mole)	972.84	1135.0 1	1297.12	1380
Water solubility at 25 °C (g/100 ml)	14.5	1.85	23.2	> 60
Applications	Oral, parenteral, topical	Oral, topical	Oral, parenteral, topical	Oral, parenteral, topical

2.2.2 Inclusion complex formation

A variety of hydrophobic compounds can be formed inclusion complexes with cyclodextrins *via* encapsulation of hydrophobic molecules (guest molecules) inside the cavity of cyclodextrin molecules (host molecules). The ability of cyclodextrin molecules to form inclusion complexes is a function of two important factors. The first factor depends on the relative size of cyclodextrins and the size of the guest or functional groups of the guest. The inclusion complexes will not be formed if the molecule of guest is big because it will slip out the cyclodextrin cavity. The second factor is the thermodynamic interactions between the components in the system. The inclusion complexation must be favourable net energetic driving force to pull the guest molecules into the host molecules. In addition, the favourable energetic interactions help shift equilibrium in inclusion complexation [20] such as:

- The water molecules (polar) displacement from the non polar cavity of host molecules.
- The increased number of forming hydrogen bonds as the displaced water returns to the larger pool
- Reduction of repulsive interactions between the aqueous medium and the hydrophobic guest molecules.
- The hydrophobic interactions increasing as the guest inserts itself into the non-polar side of host molecules.

The methods are used to form inclusion complex with cyclodextrins depending on the guest properties, equilibrium kinetics and other ingredients. The most widely method is used to prepare inclusion complex such as co-precipitation method and freeze-drying method (lyophilization).

2.2.3 Phase solubility analysis

The phase solubility method is widely used to study the inclusion complexation described by Higuchi and Connors [21].

The phase solubility is used to determine the relationship between the concentration of cyclodextrins (ligand) and the concentration of dissolved guest (substrate) (Figure 2.6). There are two main types of diagram which are types A and B. The A-type curves indicate the formation of soluble inclusion complexes when water solubility of guest increases with increasing concentration of ligand. In contrast, B-type curves indicate the formation of inclusion complexes with limited solubility in aqueous complexation medium.

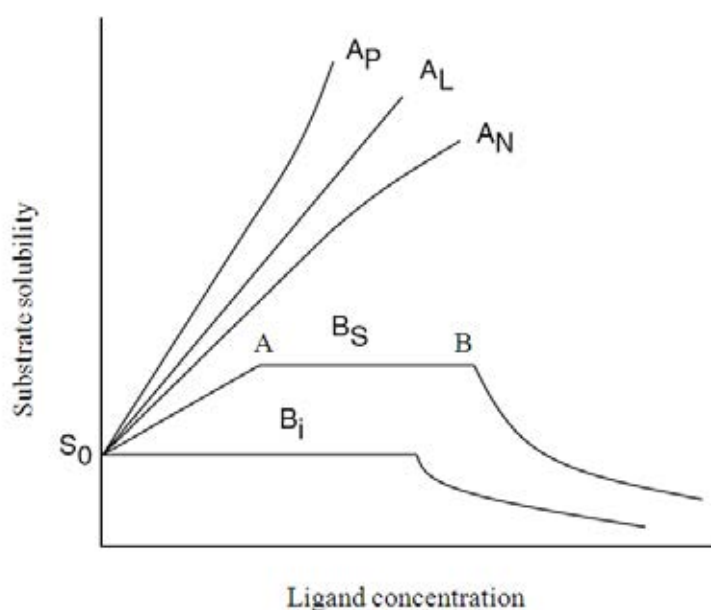


Figure 2.6 Phase solubility of A-type and B-type diagram.

In A-type curves, if an increases of guest solubility as a function of cyclodextrin concentration is linear, an A_L type is obtained and the positive deviating isotherms or negative deviating isotherms from linearity gave A_P or A_N , respectively. In addition, an A_P type is a high order inclusion complexation at higher cyclodextrin

concentrations which have more than one host molecules formed inclusion complex with the guest molecule. The B-type curves are obtained when inclusion complexes between cyclodextrin and guest molecule is not soluble. At point A (for B_S type system), the inclusion complexation reaches its limit and the guest is converted to the solid inclusion complex after point B. The derivative cyclodextrins like HPβCD often gives A-type systems due to their high water solubility.

The apparent stability constant (K_C) of 1:1 is able to calculate as the following equation:

$$K_{1:1} = \frac{\text{Slope}}{S_0(1-\text{Slope})}$$

Where S_0 is the guest solubility in the absence of cyclodextrin and slope is obtained from phase solubility diagram. The K_C value of many inclusion complexes between cyclodextrin and hydrophobic guest compound is in the range of 200 to 5,000 M^{-1} , indicating adequate to improve the water solubility of low water solubility compound [22].

However, the phase solubility diagrams do not verify inclusion complexes formation. They only describe how the increasing concentration of cyclodextrin influences guest solubility. The phase solubility studies have to be compared with other experimental to distinguish between non inclusion complex and inclusion complex such as UV/Vis spectroscopy, NMR, FTIR, DSC, and XRD.

For examples, Zhang *et al.* [23] prepared inclusion complex of caffeic acid with HPβCD and studied its formation by UV/Vis, NMR, and fluorescence spectroscopy. The water solubility was increased by 1:1 ratio of inclusion complex with HPβCD according to the phase solubility diagram. The characterized its formation confirmed that caffeic acid can be included in HPβCD cavity.

Yang *et al.* [24] studied inclusion complex between HPβCD and anti-malarial artemether. It was found that its inclusion complex was successfully prepared by the suspension method and inclusion complex was characterized by NMR, XRD

and thermal analysis to confirm its formation. The inclusion complex can be formed and the host-guest system of artemether with HP β CD showed an increase in water solubility and gave an A_L type (Figure 2.7) phase solubility diagram at K_{1:1} with 220 M⁻¹. The bioavailability enhancement for artemether was approximately 1.81-fold.

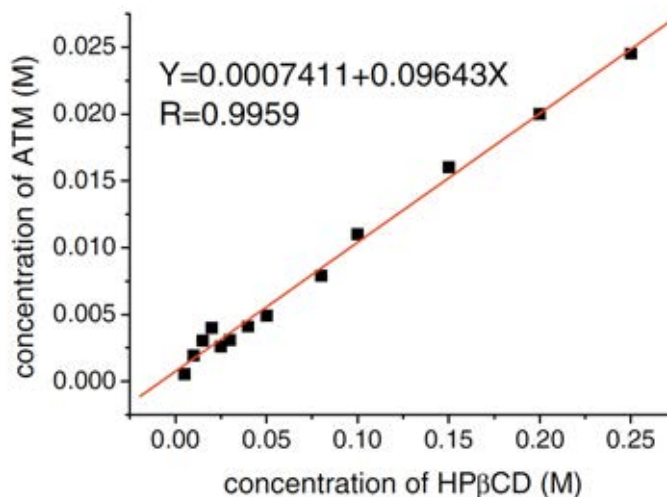


Figure 2.7 A_L type of phase solubility of Artemether/HP β CD host-guest system.

2.2.4 Inclusion complex of flavonoids and other active compounds with cyclodextrins

Most active compounds such as flavonoids have a variety of bioactivities but their use in pharmaceutical field in food and medicine are limited due to their low water and oil solubility properties. Therefore, their complexation with cyclodextrins may be used to improve water solubility and may be potentially useful for application as herbal medicines or health promoting products.

In recent years, the natural cyclodextrins (α -, β -, and γ -cyclodextrins) complexation have been successfully used to enhance the water solubility, stability, and bioavailability of many active compounds. For examples, formation of inclusion complex with α -cyclodextrin can increase the water solubility of a carotenoid bixin. It was found that its complexation is useful and efficient mechanism for protection of

carotenoid against several environmental such as ozone, air, temperature, and light [25].

Ficarra and his colleagues [26] studied inclusion complexation between β -cyclodextrin and flavonoides; hesperetin, hesperidin, naragin, and naringin, by NMR, FTIR, DSC, and XRD. It was found that the formation of inclusion complexes can improve their water solubility.

Rezende *et al.* [27] reported the inclusion complex of flavonoid dioclein. The inclusion complex of this compound with β -cyclodextrin was prepared using freeze drying method and characterized information of inclusion complex and measured its vasodilator and hypotensive effect. It was found that the 1:1 inclusion complex of dioclein/ β -cyclodextrin increased water solubility 44% when compared to free dioclein. The *in vitro* vasodilator effect was unchanged by its inclusion complex and its inclusion complex improves the hypotensive effect of dioclein by increasing its bioavailability and enables dioclein to be effective after oral administration.

Chen *et al.* [28] studied the inclusion complexation behavior of β -cyclodextrin and crassicauline A which was isolated from the traditional Chinese medicine *Aconitum crassicaule*. Crassicauline A is an excellent anti-inflammatory and analgesic. This inclusion complex was prepared by a solution ultrasonic method and was investigated in the both aqueous and solid phase by UV/Vis, NMR, FTIR, XRD, DSC, and SEM instruments. It was found that crassicauline A was included in the β -cyclodextrin cavity as shown in Figure 2.8. Moreover, the inclusion complex improved the water solubility and stability of crassicauline A.

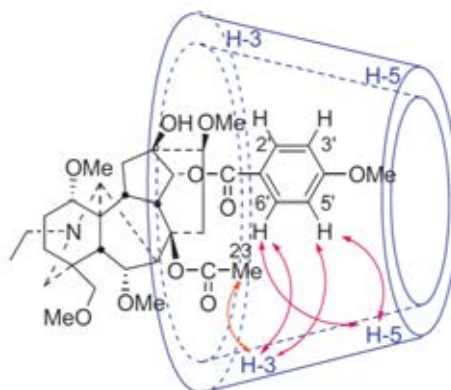


Figure 2.8 Possible inclusion mode and significant NOESY (\leftrightarrow) correlations of the crassicauline A/ β -cyclodextrin inclusion complex.

Mesplet *et al.* [29] reported the improvement of the extreme hydrophobic eflucimide using γ -cyclodextrin. It was found that the complexation of eflucimide with γ -cyclodextrins can improve the aqueous solubility of eflucimide with 1:1 stoichiometry ratio and a 20 M^{-1} formation constant.

However, the aqueous solubility of α -, β -, and γ -cyclodextrins is quite not high. Thus, there are many researches try to search for more cyclodextrin derivatives.

Recently, the derivatives of cyclodextrins have been successfully prepared to improve physicochemical properties of nature cyclodextrins. Hydroxypropyl cyclodextrin (HP β CD) is modified from β -cyclodextrin having more advantages such as high aqueous solubility (above 60%). The complexation with HP β CD has been shown to increase aqueous solubility, stability and bioavailability of poorly soluble active compounds. Moreover, HP β CD has been widely studied as a complexing agent for flavonoids.

For examples, Lin *et al.* [30] investigated the interaction of HP β CD and poorly water soluble flavonoid baicalein. The inclusion complex of baicalein with HP β CD was successfully prepared by lyophilization method (freeze-drying method). It was found that the complexation improve dissolution rate in comparison with free baicalein and improved bioavailability of baicalein.

Jullian [31] reported the improvement of water solubility of galangin using β -cyclodextrin, HP β CD, and DM β CD. The inclusion complex of galangin was formed with 1:1 stoichiometry and the solubilizing efficiency of three cyclodextrins was the order: DM β CD > HP β CD > β -cyclodextrin.

Misiuk and Zalewaska [32] studied the inclusion complexation between trazodone hydrochloride and HP β CD. Inclusion complex was prepared by co-precipitation method. It was found that the water improvement of trazodone hydrochloride with HP β CD was successfully obtained by co-precipitation method and its inclusion complex was formed with 1:1 stoichiometry ratio.

Wen *et al.* [33] improved water solubility of flavonoid naringenin by complexation with HP β CD. The physicochemical properties of naringenin/HP β CD inclusion complex were investigated by UV/Vis spectroscopy, FTIR, XRD, and DSC. The formation showed that the water solubility of inclusion complex of naraginin was enhanced from 4.38 to 1,272.31 $\mu\text{g/ml}$.

Wu *et al.* [34] prepared an inclusion complex of sulforaphane with HP β CD using co-precipitation method. The inclusion complex ratio of sulforaphane and HP β CD was found to be 1:1. FTIR, NMR, and UV/Vis spectroscopy were used to prove the formation. It was found that inclusion complex of with HP β CD can enhance the water solubility and stability of sulforaphane.

In 2011, Yang *et al.* [35] used the natural cyclodextrins (α -, β -, and γ -cyclodextrins) and its derivative (HP β CD) to improve the water solubility of the flavonoid taxifolin. The resulting inclusion complex can be formed with 1:1 stoichiometry ratio (Figure 2.9) and showed enhancement of water solubility and thermal stability of taxifolin.

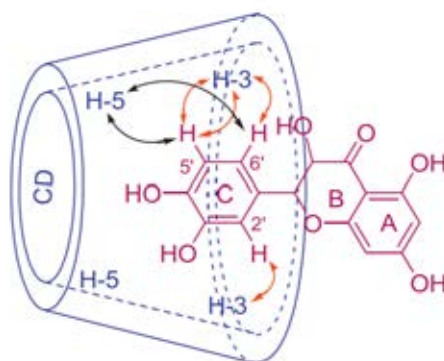


Figure 2.9 Possible inclusion mode and significant NOESY (\leftrightarrow) correlations of the taxifolin/ β -cyclodextrin, taxifolin/HP β CD, taxifolin/ α -cyclodextrin, and taxifolin/ γ -cyclodextrin inclusion complexes.

Wang *et al.* [36] reported that the inclusion complex of *trans*-ferulic acid with HP β CD was successfully prepared by freeze-drying method. The increasing water solubility and the stability of *trans*-ferulic acid were improved with HP β CD in 1:1 stoichiometry ratio.

Eid *et al.* [37] investigated the inclusion complex between zerumbone and HP β CD. The inclusion complex was successfully prepared by freeze drying method and characterized the formation of its inclusion complex by FTIR, DSC, and XRD. It was found that the solubility of zerumbone was enhanced > 30 fold after complexation.

2.3 Encapsulation by chitosan

A possible approach to enhance water solubility, stability and bioavailability of hydrophobic compounds is based on the formation of inclusion complexes with a natural or derivative cyclodextrins. However, cyclodextrins are low absorbed by gastrointestinal tract and low barrier function for oral administration, so the clinical uses of cyclodextrins have been restricted [38]. Thus, the encapsulation of cyclodextrins into polymer nanoparticles is one of the good ways used to solve these problems. The encapsulated particles are able to improve mucoadhesive properties

and also to control the release of the encapsulated drug. And chitosan is a biodegradable polymer which has been widely used for drug carrier system.

2.3.1 Encapsulation

Encapsulation is a process which active compounds are surrounded by coating to produce encapsulated capsules or spheres. The reasons in encapsulation of active compounds are to protect active compounds from environment, mark undesired properties of active compounds and control the release of active compound. If active compounds are dispersed uniformly within the polymer matrix, these are called encapsulated spheres. The capsules (or spheres) are in the micrometer, they are called micro-capsules (or spheres). If capsules (or spheres) are smaller than 1 micron, they are called nano-capsules (or spheres). For capsules, the active compounds inside the capsule are referred to as a core, whereas the wall is called a shell. The example capsules or spheres are shown in Figure 2.10.

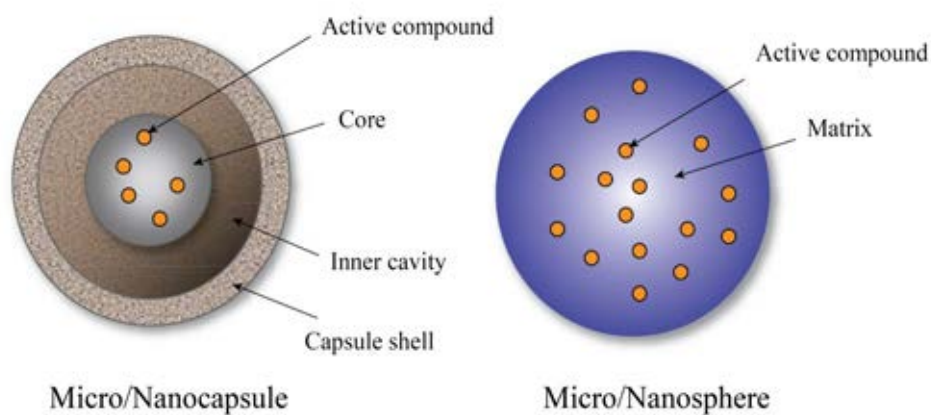


Figure 2.10 Different types of active compound micro or nanoparticles.

2.3.2 Chitosan and inclusion complex

Chitosan is cationic natural linear biopolyaminosaccharide. Chitosan is obtained by alkaline deacetylation of chitin, which present in outer structure of crustaceans such as shrimps, lobsters, crabs and prawn. Moreover, it is also found in cell wall of some fungi such as mucor and aspergillus. Chitosan has more than 50% of the degree of deacetylation of chitin consisting of copolymers of D-glucosamine and N-acetyl-D-glucosamine units linked by β -(1-4)-glycosidic linkages (Figure 2.11). Chitosan is insoluble in organic solvents and water but it is soluble in aqueous acidic solution to convert the glucosamine units into a soluble form $R-NH_3^+$.

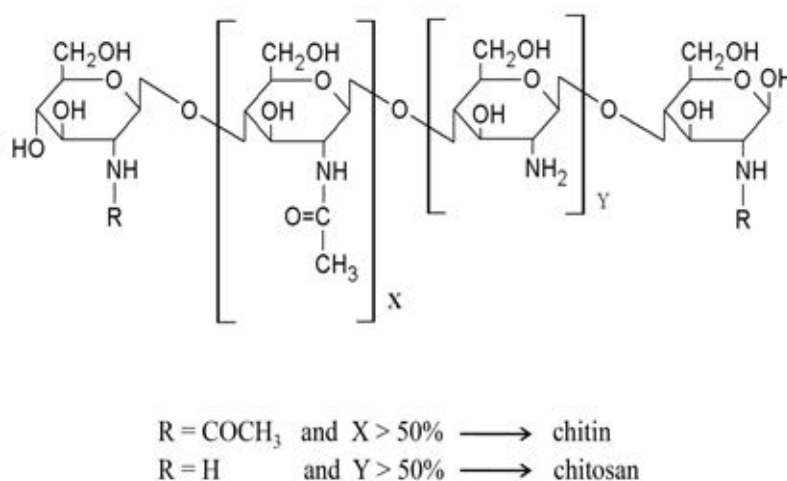


Figure 2.11 Structures of chitin and chitosan.

Chitosan has a lot of good properties such as low toxicity, biocompatibility, biodegradability, and mucoadhesion which make it suitable for use in pharmaceutical and biomedical fields. Moreover, if molecular weight and degree of deacetylation of chitosan are able to control, then it is a choice to develop micro or nanoparticles for pharmaceutical and biomedical uses. The developing chitosan micro or nanoparticles has many advantages such as their ability to control releasing of active agents, it have mucoadhesive character to increase residual time of absorption from gastrointestinal tract.

There are many reports on the preparation of chitosan micro or nanoparticles loaded inclusion complex. For examples,

Grenha *et al.* [39] reported the preparation microencapsulated nanoparticles of chitosan for lung protein delivery using spray-drying technique. The nanoparticles showed a good loading capacity of 65-80%, providing the release of 75-80% insulin within 15 min. This system may be used as drug delivery in therapy of lung local diseases.

Maestrelli *et al.* [40] reported a new nanocarrier consisting of chitosan and hydroxypropylcyclodextrin. The nanoparticles were prepared using the ionic crosslinking of chitosan with sodium tripolyphosphate in the presence of cyclodextrins. It was found that the complexation of hydrophobic drugs with cyclodextrin facilitated their entrapment into the chitosan nanoparticles and increase up to 4 and 10 times for triclosan and furosemide, respectively. In addition, the concentration of added TPP had an impact on the size of chitosan nanoparticles, when concentration of TPP went from 1.25 to 2 mg/ml, size of nanoparticles increased from 450 to 600-700 nm (Figure 2.12).

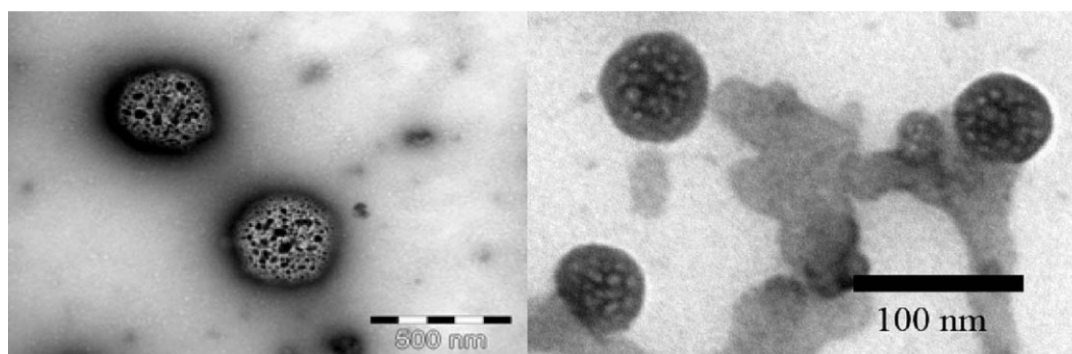


Figure 2.12 TEM images of chitosan nanoparticles with 25 mM of HP β CD (2 mg/ml TPP, top left picture; 1.25 mg/ml TPP, top right picture).

Zhang *et al.* [38] investigated the possibility of chitosan bearing β -cyclodextrin for controlling protein release, and insulin was used as protein model. The self-assembled nanocarriers showed the size in rang of 190-328 nm with high loading efficiency of 37.7%. In addition, the chitosan bearing β -CD may be used as peptides and proteins delivery for controlled the release of proteins.

Trapani *et al.* [41] studied the possibility of chitosan nanoparticles containing natural and derivatives cyclodextrins (α - and SBE_{7m}- β -CDs). The cyclodextrins encapsulation within chitosan nanoparticles were successfully prepared by an ionic cross-linking technique. The encapsulated derivatives cyclodextrin in chitosan nanoparticles have shown an improved stability in simulated intestinal fluid. Therefore, the cyclodextrins containing chitosan nanoparticles present considerable potential as nanocarriers for the oral administration of low bioavailability drug.

Vyas *et al.* [42] designed and investigated the novel HP β CD and chitosan nanocarrier for effective delivery of poorly water soluble drug simvastatin. It was found that increasing the amount of HP β CD/drug inclusion complex, increasing the final loading of the chitosan nanoparticles. This may be due to the increased solubility of simvastatin in the presence of HP β CD. *In vitro* release of loaded drug showed initial fast release followed by a delayed release pattern.

In 2011, Jingou *et al.* [43] prepared chitosan/cyclodextrin nanoparticles loading with hydrophilic and hydrophobic drug by the ionotropic gelation method. The average size of chitosan/cyclodextrin nanoparticles ranged from 308.4 ± 15.22 to 369.3 ± 30.01 nm (Figure 2.13) with drug encapsulation efficiencies of 2.48 ± 0.07 and $2.64 \pm 0.18\%$ for methotrexate and calcium folinate, respectively.

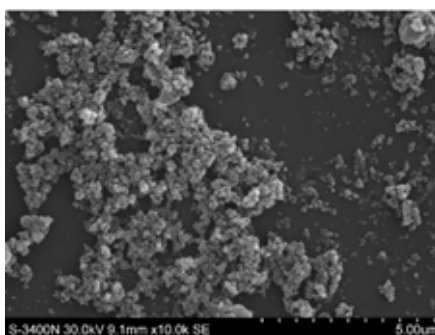


Figure 2.13 SEM image of methotrexate and calcium folinate loaded chitosan/ β -cyclodextrin nanoparticles.

2.3.3 Ionic gelation and ultrasonication method

There are many processes of preparation of chitosan micro or nanoparticles. The major processes are

- Spray-drying
- Ionotropic gelation
- Emulsion cross-linking
- Emulsion droplet coalescence method
- Coacervative/precipitation
- Reverse micellar method
- Sieving method.

However, this work is focused on a method for preparing nanoparticles by using ionotropic gelation and ultrasonication method. Ionotropic gelation is a simple and very mild method. The gelation is occurred by chemical cross-linking between chitosan and negatively charged species such as sodium tripolyphosphate, glutaraldehyde, and sodium sulfate. Sodium tripolyphosphate (TPP) is a polyanion which has been widely used due to very good cross-linkers and non-toxicity (Figure 2.14).

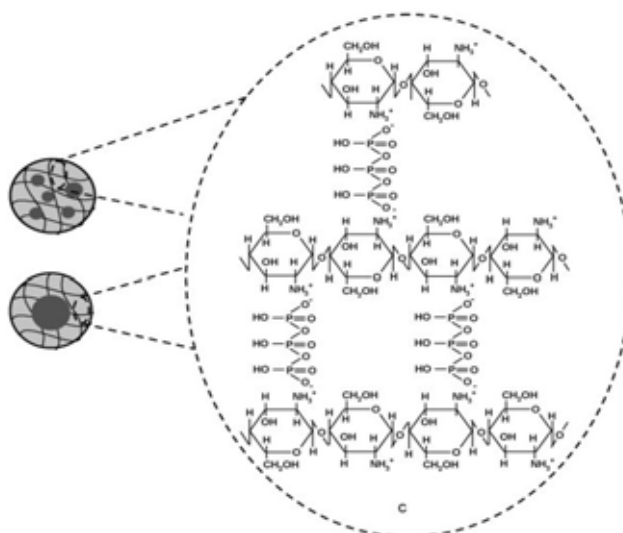


Figure 2.14 Chemical structure of chitosan ionically crosslinked with TPP [44].

Drug could be loaded into chitosan nanoparticles by 1) during the preparation of nanoparticles (incorporation) or 2) after the formation of micro or nanoparticles (incubation). In addition, if drug is water soluble compound, it is usually mixed with the solution of chitosan before forming nanoparticles. In contrast, the water insoluble drug is usually loaded to particles after by soaking the particles with the saturated solution of drugs and can also be loaded by using the multiple emulsion technique.

In addition, ultrasonication is a tool for processing and preparation of polymer nanoparticles due to cavitation of ultrasound. Ultrasound is transmitted through physical medium by waves that compress and stretch the molecular spacing of medium through which it passes. As ultrasound cross the medium the average distance between the molecules will vary as they oscillate about their mean position. When negative pressure is large enough, the distance exceeds the minimum molecular distance required to hold the liquid intact and then the liquid breaks down and voids are created. Those voids are called cavitation bubbles. The cavitation bubbles are presented into two ways; 1) stable cavitation and 2) transient cavitation. The transient bubbles are the main phenomenon responsible for ultrasonically induced chemical or mechanical effects [45].

Additionally, the solids are present in solution, the particles sizes are diminished by solids disruption, therefore the total surface increase in contact with the solvent. In general, ultrasonication method aids chemical analysis by;

- Enhancing solid liquid elemental extraction
- Speeding up solid liquid extraction of organic species
- Speeding up enzyme reactions
- Accelerating electroanalytical measurements by enhancing mass transport efficiency
- Incrementing accuracy in solid matrix dispersion technique.

In chitosan particles, the effect of ultrasonication on chitosan nanoparticles is not well understood. It is agreed that ultrasonication causes main chain scissions at

1,4-glycosidic bond without affecting the degree of deacetylation of chitosan. The degraded chitosan by the bombardment of ultrasonic radiation is caused by cavitation effect. The cavitation effect resulted in the small degraded molecule of chitosan which it resulted in small gelation chitosan/TPP nanoparticles [46]. However, low ultrasonic energy is effective in breaking up aggregates and in reducing the particle size and polydispersity of chitosan nanoparticles.

There are some studies reported the effect of ultrasonication on chitosan nanoparticles. For examples, Tang *et al.* [47] prepared chitosan nanoparticles using ionotropic gelation and ultrasonication method. The chitosan nanoparticles had mean size of 382 nm, polydispersity of 0.53 and zeta potential of 47 mV. This study indicated that the bombardment of ultrasonic radiation was able to decrease the mean diameter and polydispersity of the chitosan nanoparticles.

Tsai *et al.* [48] studied cavitation effect versus stretch effect resulted in chitosan nanoparticles. chitosan nanoparticles were prepared by ionotropic gelation and treated by ultrasonic and mechanical shearing. It was found that the higher solution temperature, the lower viscosity of solution that facilitates the sporadic cavitation effect exerted on chitosan producing smaller molecular weight fragment than that produced by stretching effect. Hence, the mean particle size prepared by cavitation effect is smaller than that prepared by tearing effect.

2.3.4 Controlled release behavior of drug from chitosan particles

Controlled release system offers many advantages and can improve many treatments. Controlled release may lead to an increased efficiency of labile drugs. The released from the dosage form, drug must pass through several physiological barriers before reaching the site of action and much then survive metabolic and chemical attacks. Labile drug may lose activity due to the local tissue environment. Controlled release dosage form can control the rate of drug delivery, the target area of drug administration and maintain therapeutic levels of drug with narrow fluctuations. That is able to reduce toxic or undesirable side effects of drug. The plasma concentration of

drug released from controlled release dosage form fluctuates within the therapeutic range over a long period of time (Figure 2.15). That makes it possible to reduce the frequency of drug administration to encourage patients to comply with dosing instructions [49].

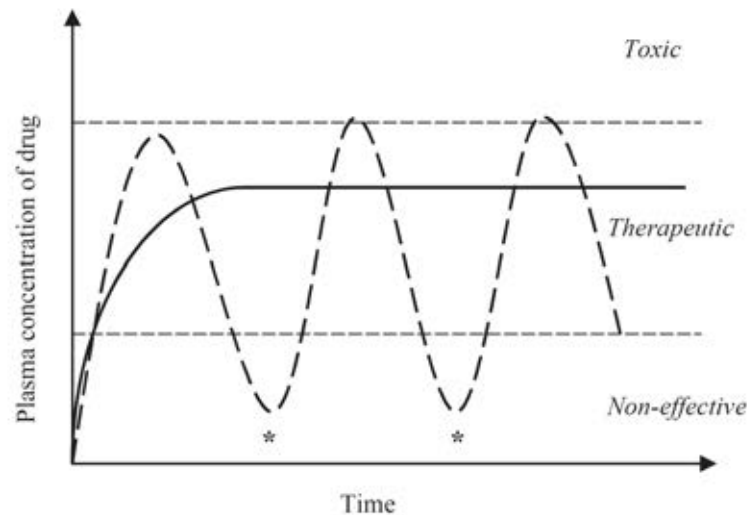


Figure 2.15 The plasma concentration of drug in the patient as a function of time after administration; (----) traditional delivery system with repetitive administration (*), (—) prolonged delivery system.

In addition, controlled release depends on the extent of cross-linking, morphology, size, drug properties, and also pH for *in vitro* release. The drug from chitosan particulate system can be released by three mechanisms (Figure 2.16) [50]. In many cases, the release of drug follows more than one mechanism, as following:

- Drug release from the surface of particles
- Diffusion through the swollen network
- Release due to chitosan erosion

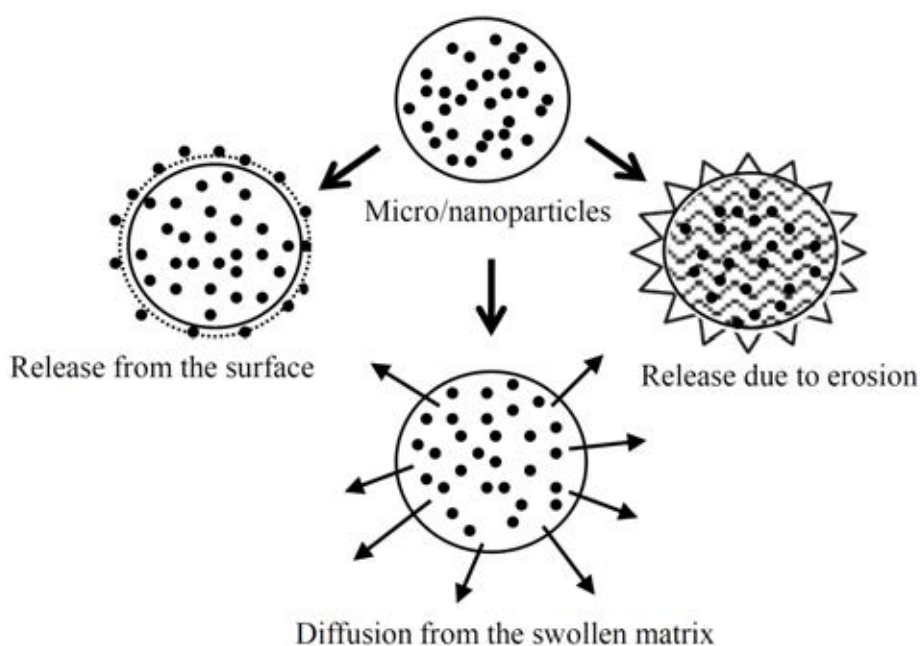


Figure 2.16 Mechanism of drug release from particulate systems.

Krauland and Alonso [51] prepared chitosan/cyclodextrin nanoparticles as macromolecular drug delivery system. The nanoparticles were prepared *via* ionic gelation. Insulin and heparin were used as model drug. *In vitro* release profile, it was found that insulin was very fast released of 84-97% within 15 min and heparin was slow released of 8.3-9.1% within 8 h. This result may be considered as nanocarriers for fast or slow drug delivery of macromolecules.

Ammar *et al.* [52] studied chitosan/cyclodextrin as drug delivery system. The nanoparticles were prepared using ionotropic gelation for the encapsulation of a model drug, sulindac. It was found that the rate of release was fast at the first hours and 55-90% being released after 3 h. The prepared nanoparticles suggest that chitosan/cyclodextrin nanoparticles showed the high percent of drug release.

CHAPTER III

EXPERIMENTAL

3.1 Chemicals and materials

- 5,7-dimethoxyflavone was isolated from *Kaempferia parviflora* according to the procedure reported by Sawasdee *et al.* [3]
- α -Cyclodextrin with \overline{M}_w of 972.84 g/mol, analytical grade (Sigma-Aldrich, USA)
- β -Cyclodextrin with \overline{M}_w of 1135.01 g/mol, analytical grade (Sigma-Aldrich, USA)
- γ -Cyclodextrin with \overline{M}_w of 1297.12 g/mol, analytical grade (Sigma-Aldrich, USA)
- (2-Hydroxypropyl)- β -cyclodextrin with \overline{M}_w of 1380 g/mol, analytical grade (Sigma-Aldrich, Singapore)
- Chitosan with \overline{M}_w of 120 kDa and a degree of deacetylation (DD) of 95% (Seafresh Chitosan (Lab) Company Limited, Thailand)
- Ethanol 95% (EtOH), analytical grade (Merck, Germany)
- Dichloromethane (CH₂Cl₂), analytical grade (Merck, Germany)
- Sodium tripolyphosphate (Na₅P₃O₁₀), analytical grade (Sigma-Aldrich, USA)
- Acetic acid, (Merck, Germany)
- Hydrochloric acid fuming (HCl), analytical grade (Merck, Germany)
- Cellulose dialysis membranes \overline{M}_w cut off at 3,500 Da (Spectrum Laboratories Inc.)
- Cellulose dialysis membranes \overline{M}_w cut off at 11,011 Da (Sigma-Aldrich, Germany)
- 0.45 μ m Nylon filter (Vertical Chromatography Co, Ltd)
- Potassium dihydrogen phosphate (KH₂PO₄ anhydrous), analytical grade (Merck, Germany)

- Sodium hydrogen phosphate (Na_2HPO_4 anhydrous), analytical grade (Merck, Germany)
- Sodium chloride (Carlo Erba Reactifs SA)
- Potassium chloride (Carlo Erba Reactifs SA)

3.2 Instruments

Table 3.1 Instruments

Instruments	Manufacture	Model
UV/Vis spectrophotometer	Agilent Technologies	Agilent 8453, C-1103A
Particle sizer	Malvern Instruments	Zetasizer Nanoseries
Fourier transform infrared spectrometer	Nicolet	6700
Freeze dryer	Labconco	FreeZone 77520
Differential scanning calorimeter	NETZSCH	DSC 204 F1
X-ray diffractometer	Philips	PW 3710 BASED
NMR spectrometer	Varian	Mercury plus 400 MHz
Scanning electron microscope	Philips	XL30CP
Transmission electron microscope	JEOL	JEM-2100 (200KV)

3.3 Method

PART I: Improvement the water solubility of 5,7-DMF

3.3.1 Preparation inclusion complexes of 5,7-DMF with different cyclodextrins

In a preliminary study, the absorption spectra of inclusion complexes between 5,7-DMF and four different cyclodextrins; α -, β -, γ -, and HP β -CDs, were evaluated. The cyclodextrin which showed the highest improvement of the water solubility (the highest absorption spectra) of 5,7-DMF will be chosen for further study. Firstly, 1.8 mg of 5,7-DMF was added into 5 ml of individual 1.25 mM CDs solutions. Subsequently, the solutions were sonicated for 20 min and shaken in a thermostatic shaking water bath at 37 ± 0.1 °C for 48 h. The solutions were then filtered (with 0.45 μ m filter) and the filtrates were analyzed the absorption spectra by Agilent 8453 UV/Vis spectrophotometer.

3.3.2 Phase solubility studies

The phase solubility of 5,7-DMF with the presence of HP β CD in deionized water was performed according to Higuchi and Connor method [21]. Briefly, an excess amount (3 mg) of 5,7-DMF was added to 10 ml of HP β CD solution at the concentrations of 0, 2, 4, 6, 8, and 10 mM (molecular weight of HP β CD is 1380). The mixtures were shaken in a thermostatic shaking water bath at 25 ± 1 °C for 48 h until equilibrium was reached. The suspensions were filtered (with 0.45 μ m filter) and measured the absorption spectra to determined the amount of 5,7-DMF by UV/Vis spectrophotometer (Agilent 8453) at 264 nm and a calibration curve of standard 5,7-DMF. The experiment was measured in triplicate. The phase solubility diagram was obtained by plotting HP β CD concentration vs. 5,7-DMF concentration.

3.3.3 Stoichiometry determination

The stoichiometry of 5,7-DMF/HP β CD inclusion complex was obtained by continuous variation (Job's plot) method [53]. Equimolar solutions of 5,7-DMF and HP β CD were mixed to a 10 ml fixed volume varying the molar ratio but containing the fixed total concentration of the species. Nine aliquots were prepared by using the

ratio volume (ml) of 2×10^{-5} M 5,7-DMF: HP β CD as 1:9, 2:8, 3:7, 4:6, 5:5, 6:4, 7:3, 8:2, and 9:1, respectively. The solutions were shaken in a thermostatic shaking water bath for 48 h and measured the absorbance by UV/Vis spectrophotometer. The difference in absorbance in the presence and absence of HP β CD ($\Delta A = A - A_0$) was plotted against molar fraction (R) of the 5,7-DMF ($R = [5,7\text{-DMF}]/([5,7\text{-DMF}] + [\text{HP}\beta\text{CD}])$).

3.3.4 Preparation 5,7-DMF/HP β CD inclusion complex

The lyophilization (freeze drying) method was used to prepare the inclusion complex of 5,7-DMF with HP β CD in 1:1 molar ratio on the basis of the results obtained from phase solubility and stoichiometry studies. The solution of 5,7-DMF dissolved in a small amount of ethanol was slowly added to the aqueous solution of HP β CD with mild stirring. The mixture was further stirred at room temperature for 96 h to reach the equilibrium between the species. The container of the solution was protected from light during stirring. The mixture was filtered through 0.45 μm filter. Then the filtrate frozen and lyophilized to obtain dried 5,7-DMF/HP β CD inclusion complex. This dried inclusion complex was stored in desiccators until uses.

The physical mixture of 5,7-DMF with HP β CD in 1:1 molar ratio was prepared by carefully mixing 5,7-DMF and HP β CD in a ceramic mortar.

3.3.5 Characterization of 5,7-DMF/HP β CD inclusion complex

3.3.5.1 Fourier-Transform infrared spectroscopy (FTIR)

The studying of functional groups on 5,7-DMF, HP β CD, 5,7-DMF/HP β CD inclusion complex, and physical mixture were performed on FTIR spectrometer. The IR spectra was recorded in the wavelength region 4000–400 cm^{-1} on ATR mode using a Nicolet 6700 and Omnic software was used to control the measurement.

3.3.5.2 Differential scanning calorimetry analysis (DSC)

DSC was used to investigate the thermal properties of 5,7-DMF, HP β CD, 5,7-DMF/HP β CD inclusion complex, and physical mixture. Which confirm not only interaction but also real inclusion complexation of 5,7-DMF and HP β CD. DSC was performed by NETZSCH DSC 204 F1. All samples were heated from 25 °C to 340 °C at heating rate of 10 K/min under nitrogen atmosphere.

3.3.5.3 X-ray diffractometry analysis (XRD)

The powder X-ray diffraction patterns of the 5,7-DMF, HP β CD, 5,7-DMF/HP β CD inclusion complex, and physical mixture were obtained using Philips PW 3710 BASED diffractometer system with Cu ($\lambda = 1.5406 \text{ \AA}$), in the range of $3^\circ \ll 2\theta \gg 50^\circ$ (voltage 40 kV, 30 mA).

3.3.5.4 NMR spectroscopy

1D and 2D NMR spectroscopy analysis were performed on Varian Mercury 400 NMR spectrometer at ambient temperature and the inclusion complex was recorded in the D₂O solvent system.

PART II: Encapsulation 5,7-DMF/HP β CD inclusion complex in chitosan nanoparticle

3.3.6 Preparation chitosan nanoparticles for characterization morphology

Chitosan nanoparticles were prepared firstly by ionotropic gelation method and then treated with ultrasonication to reduce the sizes of particles. Briefly, 0.2% (w/v) chitosan solution in 1% (v/v) acetic acid was prepared. Then 1 ml of a cross-linking agent TPP was slowly dropwised into 4 ml of under the magnetic stirring for 1 h at room temperature to obtain nanoparticles. These chitosan nanoparticles were further treated with ultrasonication equipment at the amplitude of 50 by varying the duration time at 5, 10, 15, and 20 min. Nanoparticles were isolated by centrifugation

at 16,000 g for 30 min. The residues under supernatant were kept and resuspended in deionized water before characterized by SEM.

3.3.7 Preparation 5,7-DMF/HP β CD loaded chitosan nanoparticles for characterization morphology

5,7-DMF/HP β CD inclusion complexes loaded chitosan nanoparticles (ICCSNP) were prepared as previous described in 3.3.6 with the exception that 2 ml of (0.2%, 0.4%, and 0.8% w/v) an aqueous solution of 5,7-DMF/HP β CD inclusion complex was added into the 2 ml of chitosan solution (0.4% w/v). The time range (5 min) for ultrasonication was obtained from the appropriate result of 3.3.6.

3.3.8 Preparation 5,7-DMF/HP β CD loaded chitosan nanoparticles for *in vitro* release studies

ICCSNP were prepared as previous described in 3.3.7 with the exception of centrifugation. The ICCSNP suspension was dialyzed in deionized water using a dialysis bag (cellulose dialysis membranes, \overline{M}_w cut off of 11,011 Da) under the magnetic stirring for 2 h. The non-encapsulation 5,7-DMF/HP β CD inclusion complex was separated out from the dialysis bag. The nanoparticle suspension in a bag was further frozen and lyophilized until dry.

3.3.9 Characterization of nanoparticles

The morphology of nanoparticle was performed by scanning electron microscopy (SEM, Philips XL30CP) and transmission electron microscopy (TEM, JEM-2100 (200KV)). For SEM measuring, nanoparticles were placed on the stub and coated with gold under vacuum. For TEM measuring, 2% (w/v) of phosphotungstic acid was used for staining the samples. The staining samples were placed on copper grids (with Formvar[®] films) and dried for viewing.

The particle size, size distribution, and zeta potential of nanoparticles were determined by dynamic light scattering using Zetasizer Nanoseries ZS model S4700 (Malvern Instrument, UK).

3.3.10 Entrapment efficiency and loading capacity

An indirect method was used for calculation of entrapment efficiency and loading capacity of 5,7-DMF/HP β CD inclusion complex loaded chitosan nanoparticles [54]. Briefly, 3 ml of a freshly suspension of ICCSNP was placed in a dialysis bag (cellulose dialysis membranes, \overline{M}_w cut off of 3,500 Da) and immersed in 15 ml of deionized water under magnetic stirring at room temperature. The samples were withdrawn from dialysis medium (3 ml) and replaced with equal volumes of fresh deionized water at appoint of time interval. The withdrawn samples were analyzed the amount of inclusion complexes by measuring their absorbance using Agilent 8453 UV/Vis spectrophotometer at $\lambda_{\max} = 264$ nm. The experiments were carried out in triplicate. When concentration of the inclusion complex from the withdraw solution did not increase it was assumed that non entrapped inclusion complexes (free inclusion complexes) in both of in dialysis bag and dialysis medium were completely equilibrium. Therefore, the entrapment efficiency and loading capacity were calculated as follows:

$$EE\% = \frac{\text{Total amount of inclusion complex} - \text{Amount of free inclusion complex}}{\text{Total amount of inclusion complex}} \times 100$$

$$LC\% = \frac{\text{Total amount of inclusion complex} - \text{Amount of free inclusion complex}}{\text{Nanoparticles weight}} \times 100$$

3.3.11 *In vitro* release studies

Preparation of buffer medium

Hydrochloric acid (HCl) with pH of 1.2 was prepared and adjusted pH to 1.2 with 1 M NaOH or 1 M HCl.

Phosphate buffered saline (PBS) with pH of 7.4 was prepared by dissolving 8 g NaCl, 0.2 g KCl, 1.44 g Na₂HPO₄ and 0.24 g KH₂PO₄ in approximately 1000 ml of deionized water and adjusted pH to 7.4 with 1 M NaOH or 1 M HCl.

In vitro release studies

The inclusion complexes were studied their releasing behavior from CCSNP in HCl (pH 1.2) and PBS (pH 7.4) by dialysis membranes diffusion technique.

Briefly, the known loading ICCSNP was added into 4 ml of HCl medium (or PBS). The mixture was placed into a dialysis bag (cellulose dialysis membranes, \overline{M}_w cut off of 3,500 Da) and immersed in 14 ml of HCl medium (or PBS) with shaking in a thermostatic shaking water bath at 37 ± 0.1 °C. The samples were taken and replaced with equal volumes of fresh HCl medium (or PBS) at appoint a time interval. The amount of released inclusion complex was determined by measuring it absorbance using UV/Vis spectrophotometer (Agilent 8453) at $\lambda_{\max} = 264$ nm and experiments were performed in triplicate. The percentages of inclusion complex release were calculated as follow:

$$\% \text{ release} = \frac{\text{Amount of inclusion complex from release}}{\text{Amount of inclusion complex before release}} \times 100$$

3.3.12 Statistical analysis

All experiments were carried out in triplicate and the results are shown as mean \pm SD. Microsoft Excel (Microsoft Corporation) with one-way ANOVA was used to calculate statistical analysis ($P < 0.05$, indicating statistical significance).

CHAPTER IV

RESULTS AND DISCUSSION

This research study was divided into two parts. The first part reported the water solubility improvement of 5,7-DMF *via* the inclusion complexation of 5,7-DMF with HP β CD and the second part presented the encapsulation of inclusion complex in chitosan nanoparticle *via* the ionotropic gelation and ultrasonication method.

PART I: Improvement water solubility of 5,7-DMF

4.1 Preliminary studies

In general, cyclodextrins which have a structure consisting of a hydrophobic cavity and a hydrophilic outer surface have been used to improve the water solubility, bioavailability and stability of many hydrophobic compounds *via* inclusion complexation [30]. However, the inclusion complexation of 5,7-DMF with cyclodextrins have not been reported yet. Therefore, the aim of this study was to improve the water solubility of 5,7-DMF with cyclodextrins.

According to the procedure in section 3.3.1, the water solubility improvement of 5,7-DMF with α -, β -, γ -, and HP β -CD was investigated. The results in Figure 4.1 indicated that all cyclodextrins can enhance the aqueous solubility of 5,7-DMF as the absorbance intensity increase. Among of them, the inclusion complexation of 5,7-DMF with HP β CD showed the highest absorbance. Hence in this study, HP β CD was chosen to prepare the inclusion complexes with 5,7-DMF.

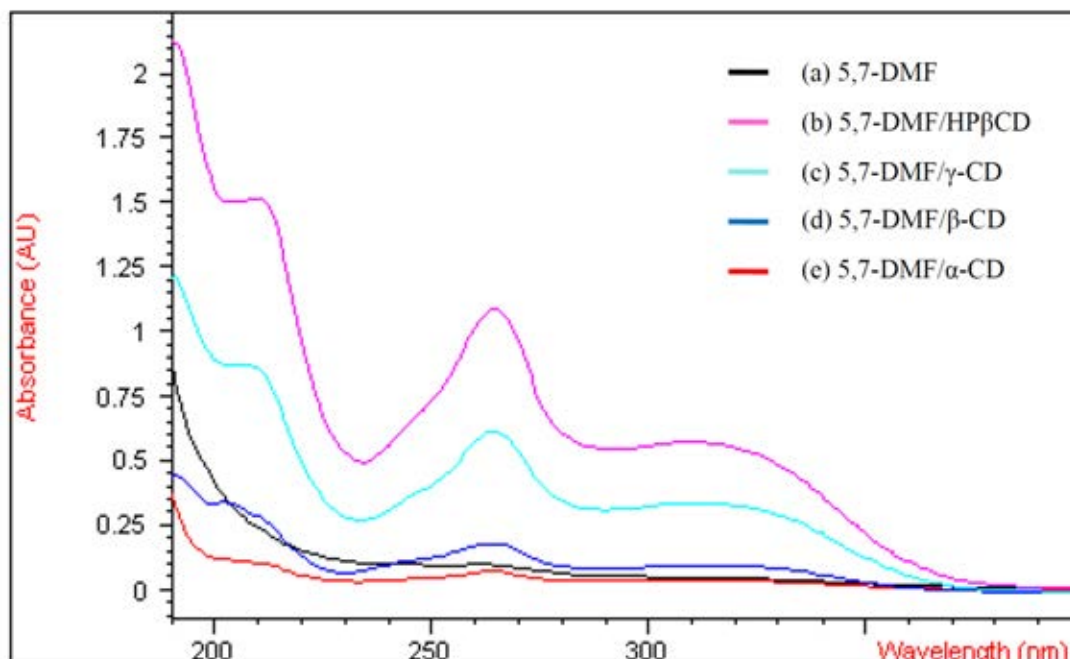


Figure 4.1 UV spectra of (a) free 5,7-DMF and 5,7-DMF in the presence of (b) HP β CD, (c) γ -CD, (d) β -CD, and (e) α -CD.

4.2 Inclusion complex of 5,7-DMF with HP β CD

The phase solubility and the stoichiometry of 5,7-DMF/HP β CD inclusion complex were determined by UV/Vis spectrophotometer and characterized the formation of 5,7-DMF/HP β CD inclusion complex by FTIR, DSC, XRD, 1D, and 2D NMR spectroscopic analysis.

4.2.1 Phase solubility studies

Phase solubility diagram is a widely method that used to elucidate the effect of cyclodextrin complexation on the solubility of hydrophobic drug.

The solubility of 5,7-DMF with varying concentration of HP β CD and its phase solubility diagram are presented in Table 4.1 and Figure 4.2, respectively. The diagram showed that the solubility of 5,7-DMF increased as the HP β CD concentration increased due to inclusion complexation of 5,7-DMF with HP β CD. The

phase solubility of 5,7-DMF/HP β CD system within the range of concentration studied displayed a A_L type (with a slope lower than 1) which indicated the formation of a 1:1 stoichiometry of 5,7-DMF and HP β CD according to Higuchi and Connors [21]. The apparent stability constant (K_{1:1}) was calculated by the following equation:

$$K_{1:1} = \frac{\text{Slope}}{S_0(1-\text{Slope})}$$

The K_{1:1} for 5,7-DMF/HP β CD inclusion complex was found to be 1840 M⁻¹. The value of K_{1:1} is most often found between 200 and 5000 M⁻¹ [22], thus the value of K_{1:1} for 5,7-DMF/HP β CD inclusion complex indicated a high tendency of 5,7-DMF to enter the cavity of HP β CD.

Table 4.1 Solubility of 5,7-DMF in 0-10 mM HP β CD concentration at 25 ± 1 °C, n=3

Concentration of HP β CD (mM)	Concentration of 5,7-DMF (mM) (average ± SD)
0	0.0128 ± 0.01
2	0.0582 ± 0.01
4	0.1002 ± 0.02
6	0.1490 ± 0.01
8	0.1978 ± 0.02
10	0.2460 ± 0.02

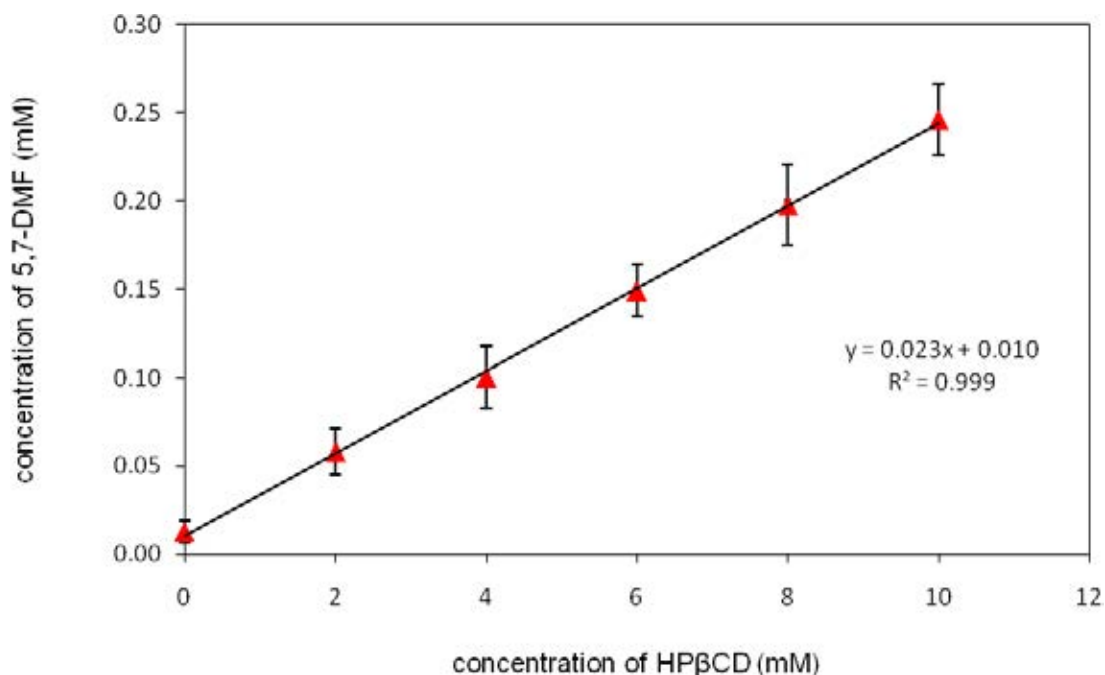


Figure 4.2 Phase solubility diagram for the 5,7-DMF/HPβCD system at 25 ± 1 °C, $n=3$

4.2.2 Stoichiometry determination

According to the continuous variation (Job's plot) method, when a physical parameter related to the complex concentration for sample setting with continuously varying molar fraction of guest and host molecule can be measured. The maximum of complex concentration is present in the sample where the molar ratio R corresponds to the stoichiometry of complexation. Figure 4.3 showed the Job's plot which the maximum adsorbance of 5,7-DMF/HPβCD was observed for $R=0.5$, indicating that inclusion complex of 5,7-DMF with HPβCD in the main stoichiometry is 1:1 molar ratio in aqueous solution in accordance with the result of stoichiometry obtained by the phase solubility study.

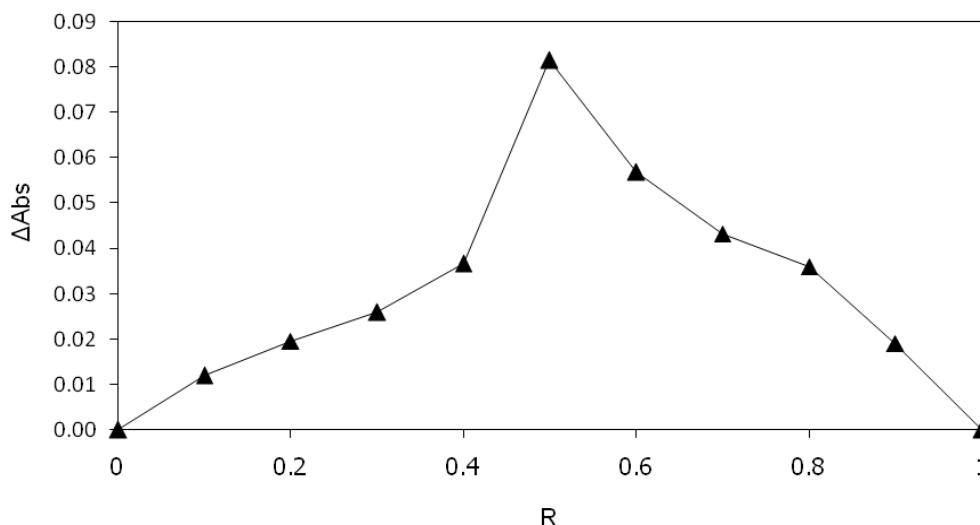


Figure 4.3 Continuous variation plot for the 5,7-DMF/HP β CD system from absorbance measurements ($R = [5,7\text{-DMF}]/([5,7\text{-DMF}]+[\text{HP}\beta\text{CD}])$).

4.2.3 Characterization 5,7-DMF/HP β CD inclusion complex

4.2.3.1 Fourier-transform infrared spectroscopy (FTIR)

The FTIR spectra was used to confirm the formation of complex and interaction between 5,7-DMF and HP β CD by comparing the complex with a physical mixture and pure substance. Changes or shifts in the characteristic bands of guest molecules confirmed the existence of new compound with different spectroscopic bands.

The FT-IR spectra of 5,7-DMF, HP β CD, inclusion complex, and physical mixture are presented and the complete band assignments are shown in Figure 4.4 and Table 4.2, respectively. A strong adsorption band at 1645 cm^{-1} , 1345 cm^{-1} , 1116 cm^{-1} , and 1156 cm^{-1} of the 5,7-DMF were assigned to the $\nu(\text{C}=\text{O})$, $\delta(\text{C-H})$ from CH_3 , $\nu(\text{C-O})$, $\delta(\text{C-CO-O})$, respectively. These bands disappeared in the spectra of inclusion complex indicating that these bands were entrapped into the cavities of HP β CD. These results suggested an interaction between 5,7-DMF and HP β CD. However, the existence of 5,7-DMF in the inclusion complex is confirmed by the bands at 1644

cm^{-1} and 1349 cm^{-1} . In addition, the adsorption spectra of the physical mixture (Figure 4.4d) did not differ significantly from the individual component.

Table 4.2 wavenumbers (cm^{-1}) and assignments for the bands observed in the FTIR spectra of 5,7-DMF, HP β CD and inclusion complex.

5,7-DMF	HP β CD	Inclusion complex
3074: ν (C-H) from aromatic ring	3333: ν (O-H)	3334: ν (O-H)
2942 and 2839: ν (C-H) from CH_3	2928: ν (C-H)	2927: ν (C-H)
1645: ν (C=O)	1456: δ (C-H) from CH_2 and CH_3	1644: ν (C=O)
1605, 1575 and 1487: ν (C=C) from aromatic ring	1366: δ (C-H) from CH_3	1456: δ (C-H) from CH_2 and CH_3
1452 and 1345 δ (C-H) from CH_3	1339: coupled δ (C-C-H), δ (C-O-H), δ (H-C-H)	1608: ν (C=C) from aromatic ring
1254, 1116 and 1057: ν (C-O)	1151 and 1079: ν (C-O), ν (C-C), δ (C-O-C)	1349: δ (C-H) from CH_3
1156: δ (C-CO-C)	1023: δ (O-C-H), δ (C-C-H), δ (C-C-O)	1152 and 1080: ν (C-O), ν (C-C), δ (C-O-C)
820, 763 and 731 : δ (C-H) out of plane bending from aromatic ring	947: skeletal vibration involving α -1,4 linkage	1024: δ (O-C-H), δ (C-C-H), δ (C-C-O)
	850: δ (C-C-H), ν (C-O), ν (C-C) from anomeric vibration	947: skeletal vibration involving α -1,4 linkage
		853: δ (C-C-H), ν (C-O), ν (C-C) from anomeric vibration

ν , stretching vibration; δ , bending vibration

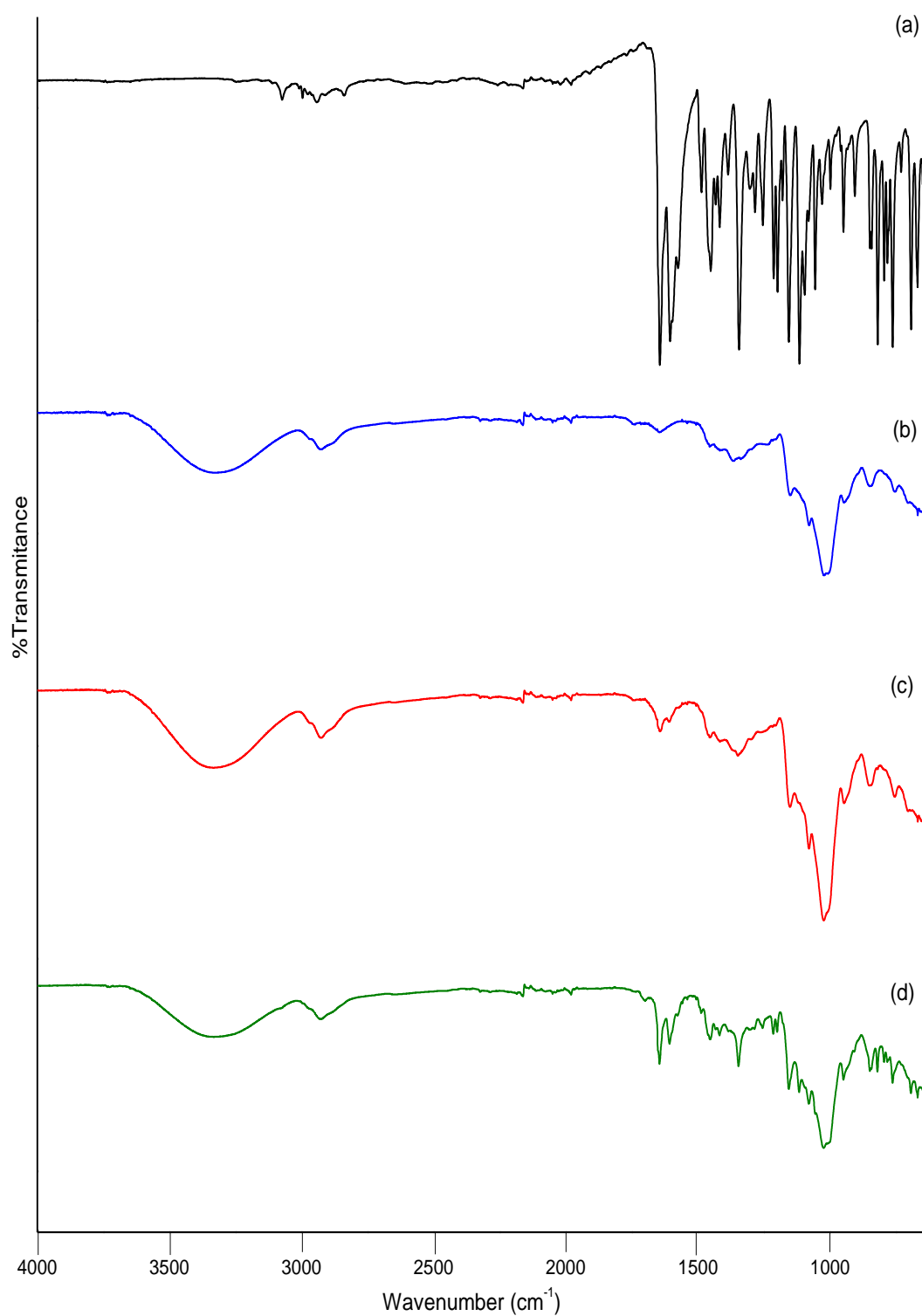


Figure 4.4 The FTIR spectra of (a) 5,7-DMF (b) HPβCD (c) inclusion complex and (d) physical mixture.

4.2.3.2 Differential scanning calorimetry analysis

The differential scanning calorimetry (DSC) thermogram showed the thermal properties of inclusion complex. The DSC curve confirm not only interaction but also real inclusion complexation by the shifting, broadening and the loss of guest molecule peak or presence of new peaks. In general, the formation of an inclusion complex with cyclodextrin was observed for the absence of melting endotherm of the guest molecule when guest molecule is complexed with cyclodextrin. At the guest melting temperature has not energy adsorption due to the guest is no crystalline to absorb energy as a result of surrounding of cyclodextrin molecule on the guest molecule incommode interacting with other guest molecule.

The DSC curve of 5,7-DMF, HP β CD, inclusion complex, and physical mixture are shown in Figure 4.5. In Figure 4.5(a), showed an endothermic peak at 152 °C corresponding to the melting point of 5,7-DMF. In Figure 4.5(b), showed the broad endothermic peak at 96.9 °C which corresponded to the loss of water of HP β CD and displayed the thermal decomposition peaks above 320 °C. The DSC curve of the 5,7-DMF/HP β CD inclusion complex is shown in Figure 4.5(c). The melting point of 5,7-DMF is not observable but its DSC curve showed an endothermic peak at 86.6 °C which may be indicated the interaction between 5,7-DMF and HP β CD. According to the HP β CD gave an amorphous character complex when complex was formed with hydrophobic drug. Finally, the DSC curve of the physical mixture in Figure 4.5(d) showed a combination of the thermal behaviour of both individual components.

4.2.3.3 X-ray diffractometry analysis

The powder X-ray diffraction (XRD) of the 5,7-DMF, HP β CD, inclusion complex, and physical mixture are shown in Figure 4.6. The x-ray diffraction pattern of the HP β CD in Figure 4.6(a) was amorphous due to it is the characteristic of non crystalline structure. On the contrary, the 5,7-DMF XRD diffraction pattern in Figure 4.6(b) presented the crystalline of 5,7-DMF diffraction peaks. Additionally, the non crystalline pattern of 5,7-DMF/HP β CD inclusion complex is shown in Figure 4.6(c). These result showed that the complexation with HP β CD may affect to change

crystalline nature of 5,7-DMF. The amorphous state of inclusion complex proves that the 5,7-DMF was dispersed within HP β CD cavity in a molecular state. On the other hand, some of lower intensity crystalline peaks of 5,7-DMF were still in the physical mixture that XRD pattern showed mostly of the HP β CD character in Figure 4.6(d).

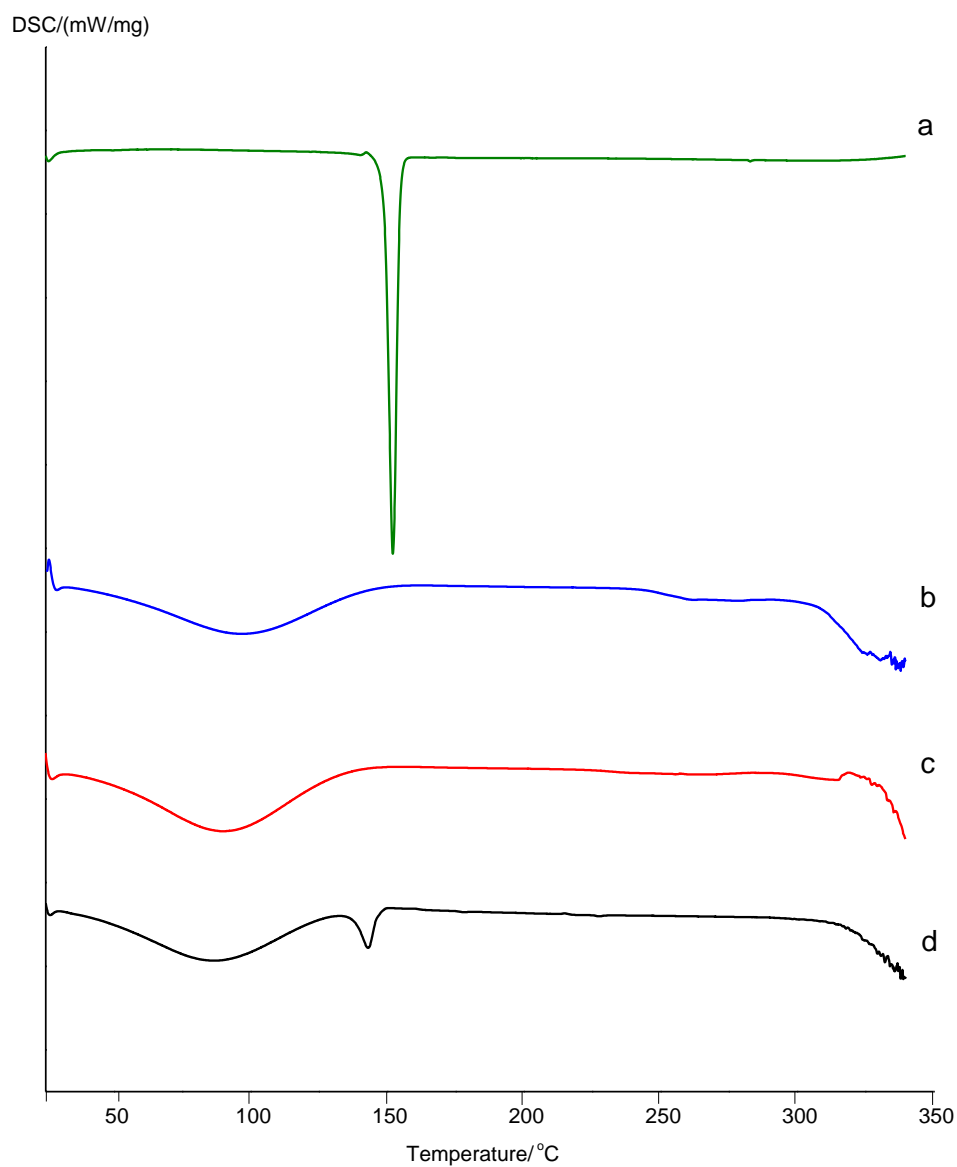


Figure 4.5 The DSC thermograms of (a) 5,7-DMF (b) HP β CD (c) inclusion complex and (d) physical mixture.

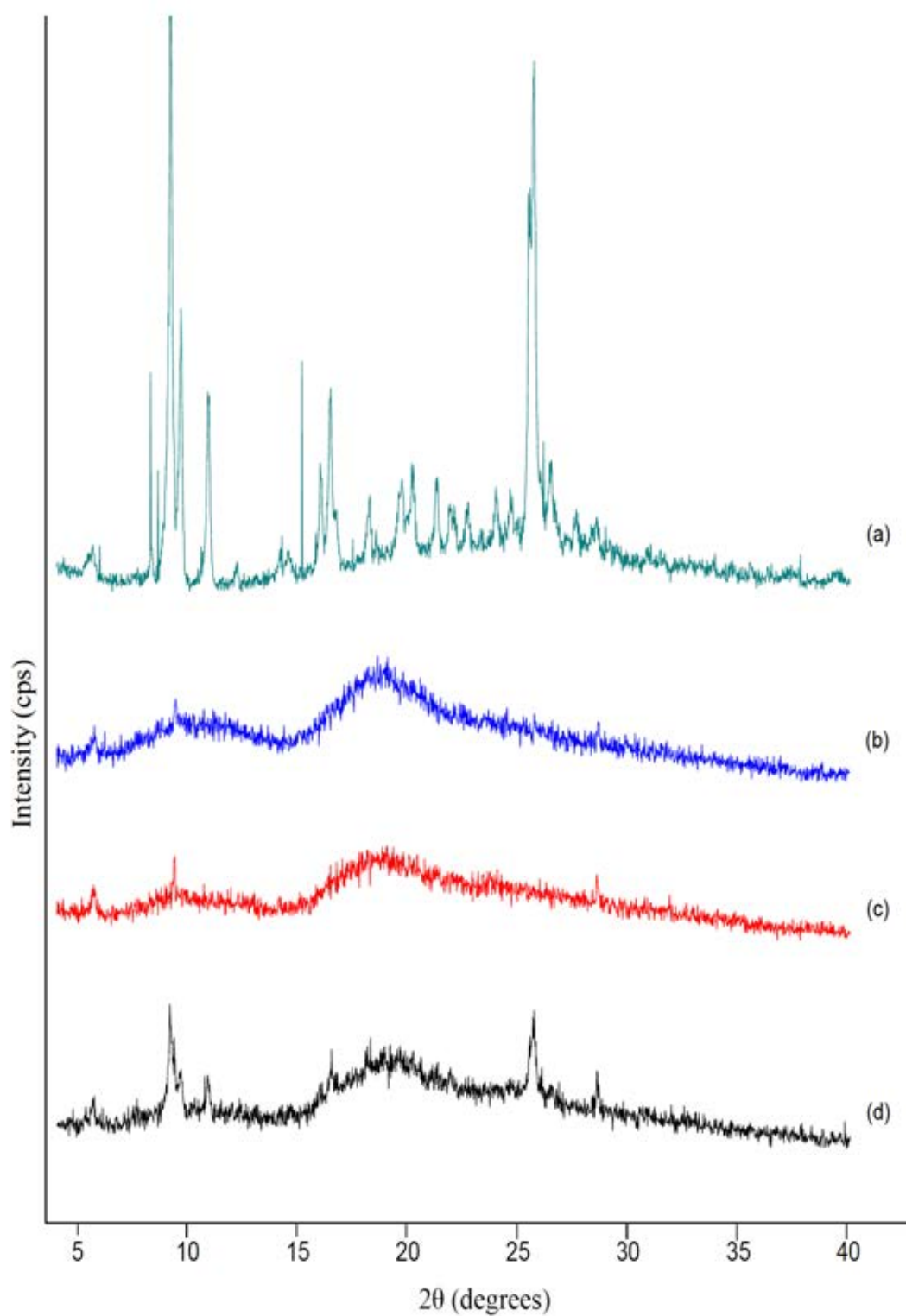


Figure 4.6 The XRD patterns of (a) 5,7-DMF (b) HP β CD (c) inclusion complex and (d) physical mixture.

4.2.3.4 NMR spectroscopy

The ^1H -NMR spectra of 5,7-DMF, HP β CD and inclusion complex are presented in Figure 4.7 and the assignments are given in Table 4.3. Due to the low solubility of 5,7-DMF in water, it was difficult to elucidate in detail of the chemical shifts of 5,7-DMF protons before and after inclusion complexation when D_2O was used as solvent. However, in this study only HP β CD proton before and after inclusion complexation can be discussed. For the chemical shifts of HP β CD, the upfield shifts of H-3 and H-5 protons may confirm the inclusion complexation between 5,7-DMF and HP β CD cavity because both the H-3 and H-5 protons are located inside the HP β CD cavity near the wide side and the narrow side respectively. These results may lead to the assumption that 5,7-DMF was included into the cavity of the HP β CD. According to the 2D NMR spectroscopy (NOESY), the NOESY spectrum of inclusion complex as can be seen from Figure 4.8 showed the cross peaks between the H-6 and H-8 protons of 5,7-DMF with H-6 and H-5 protons of HP β CD. These results indicate that the A and C rings of 5,7-DMF were included in the HP β CD cavity and a possible inclusion mode of 5,7-DMF with HP β CD is proposed in Figure 4.9.

Table 4.3 The chemical shifts (δ) of HP β CD and 5,7-DMF/HP β CD inclusion complex in D_2O where $\Delta\delta = (\delta_{\text{complex}} - \delta_{\text{free}})$.

		δ (ppm)		$\Delta\delta$ (ppm)
		HP β CD	inclusion complex	
H-1	d	4.885	4.878	-0.007
H-2	dd	3.441	3.436	-0.005
H-3	d	3.771	3.758	-0.013
H-4	dd	3.399	3.393	-0.006
H-5	m	3.681	3.644	-0.037
H-6	dd	3.681	3.675	-0.006
CH_3	dd	0.965	0.956	-0.009

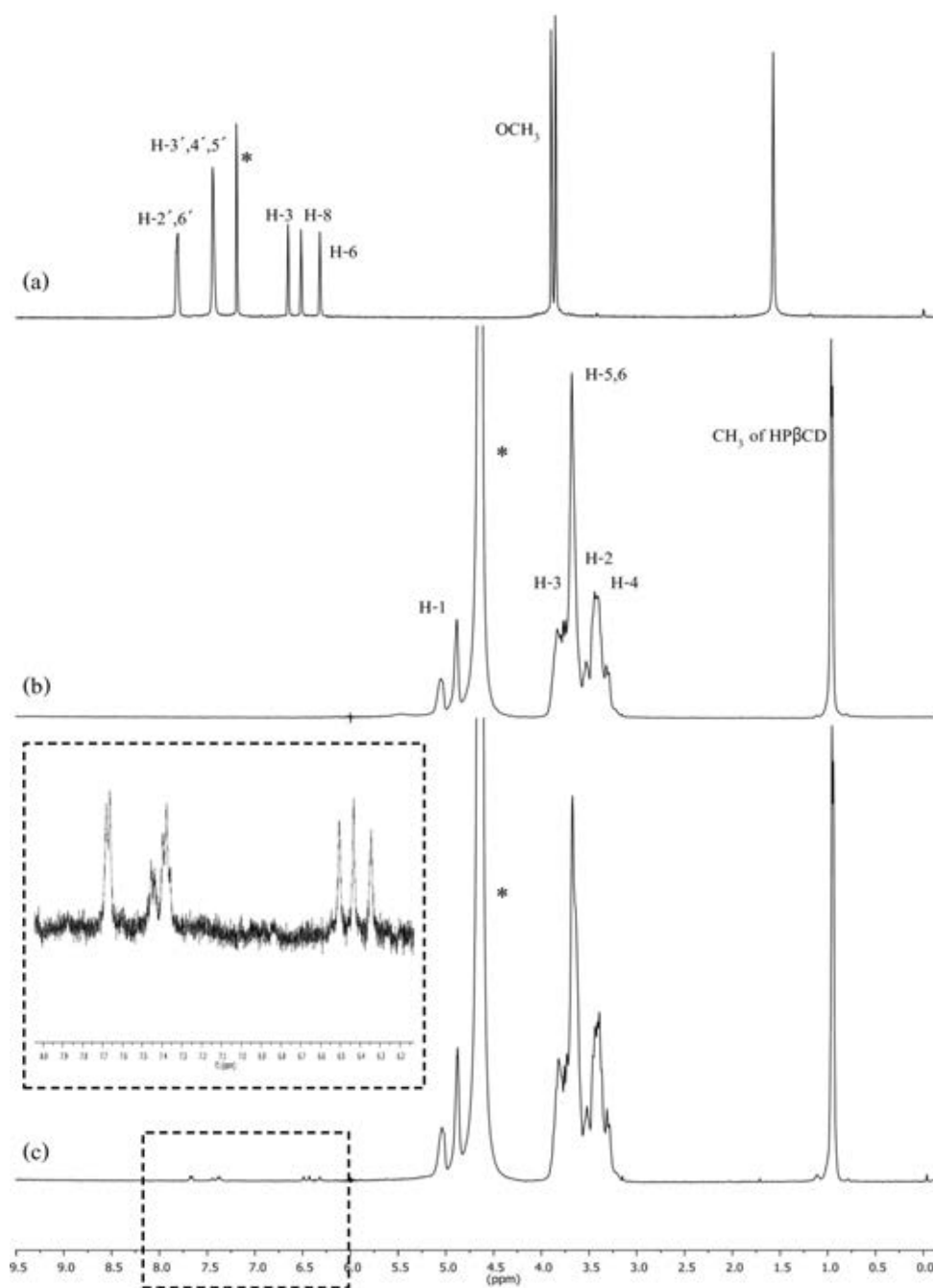


Figure 4.7 ^1H NMR spectra of 5,7-DMF in CDCl_3 and HP β CD in the absence and presence of 5,7-DMF in D_2O at 25 $^\circ\text{C}$. (a) 5,7-DMF, (b) HP β CD, (c) 5,7-DMF/HP β CD complex (asterisk highlights the solvent peak, the window shows the enlarged ^1H NMR spectrum from approximately 6-8 ppm).

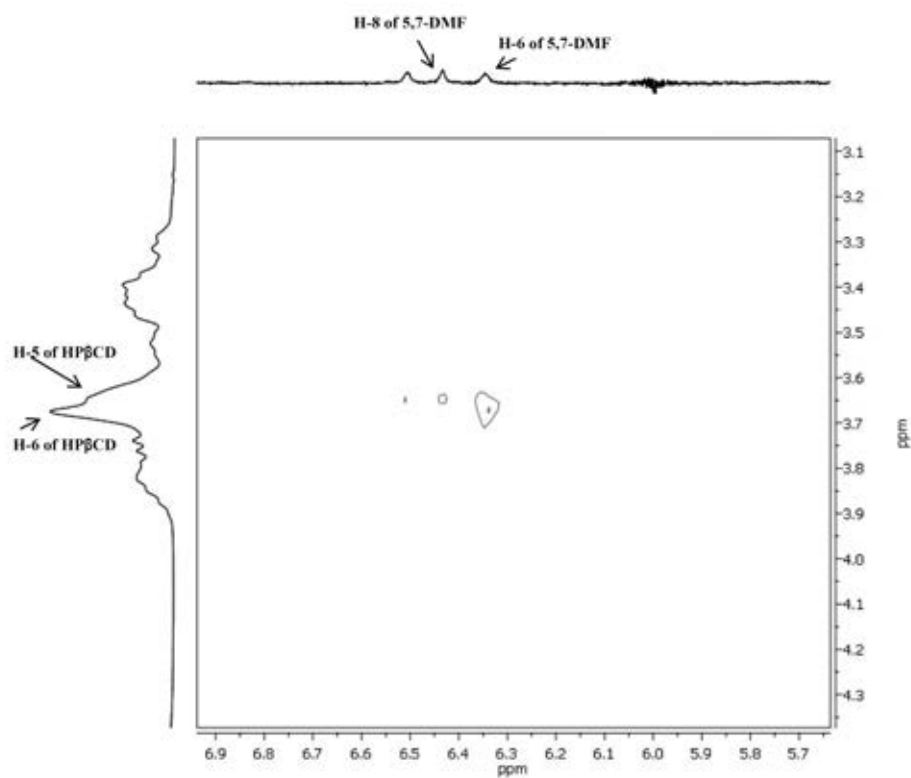


Figure 4.8 NOESY spectrum of 5,7-DMF/HPβCD inclusion complex in D₂O.

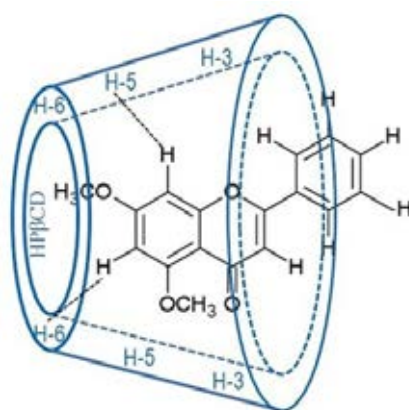


Figure 4.9 Possible inclusion mode of the 5,7-DMF/HPβCD complex.

PART II: Encapsulation 5,7-DMF/HP β CD inclusion complex in chitosan nanoparticle

4.3 Preparation chitosan nanoparticles

Using a method described by Amber Vyar *et al.* [42] with slightly modified, chitosan particles were successfully prepared by ionotropic gelation method using tripolyphosphate (TPP) as a cross-linker and then treated these particles by ultrasonication with 50% of amplitude by varying treated times.

The physicochemical properties of chitosan particles are shown in Table 4.4. The particles formed by chitosan/TPP ratio of 4:1 w/w without ultrasonication (CSNP) displayed a large particles size of 1.46 μm and high polydispersity index (PDI = 0.94) which was in agreement with a wide size distribution (Figure 4.10a). The chitosan particles treated with ultrasonication (uCSNP) displayed the lower particles sizes in a range between 189-222 nm and had low polydispersity indexes (PDI = 0.3-0.41) which were in agreement with the narrow size distributions in Figure 4.10b-4.10d. The mean particles size and polydispersity of ionotropic gelation chitosan particles decreased due to cavitation effect of ultrasonic [45]. This phenomenon was in agreement with the previous report. Tang *et al.* studied the effect of ultrasonication on the properties of chitosan and ionotropic gelation chitosan nanoparticle. It was found that the bombardment of ultrasonic radiation resulted in breaking up aggregates and decreasing in the mean particle size and polydispersity of ionotropic gelation chitosan nanoparticle [47]. However, a longer time of treated ultrasonication resulted in the larger sizes of chitosan nanoparticle. This may be due to the fact that the longer time of ultrasonication will facilitate the entanglement of some chitosan molecules to form aggregated chitosan clusters. The aggregated chitosan cluster then ionotropically gelled with TPP to form the bigger chitosan nanoparticles [48]. Additionally, the nanoparticles showed positive zeta potential due to the free positively charged amino groups of chitosan on the surface of nanoparticles.

Table 4.4 Physicochemical properties of chitosan particles following ultrasonication at specified duration time (mean \pm SD, n=3).

Ratio CS:TPP(w/w)	Amplitude	Duration (min)	Size (nm)	PDI	Zeta potential (mV)
4:1	0	0	1460 \pm 49	0.94	+52 \pm 1.8
4:1	50	5	195 \pm 3	0.31	+36 \pm 0.8
4:1	50	10	189 \pm 3	0.31	+45 \pm 1.2
4:1	50	15	222 \pm 3	0.41	+47 \pm 2.1
4:1	50	20	204 \pm 12	0.35	+46 \pm 1.8

Morphology studies of CSNP and uCSNP were recorded by scanning electron microscopy (SEM). SEM images (Figure 4.11) confirmed the spherical shape and smooth particles. The mean sizes of CSP from SEM were similar with the size obtained from particle sizer but those of uCSNP particles appear to be a little aggregated.

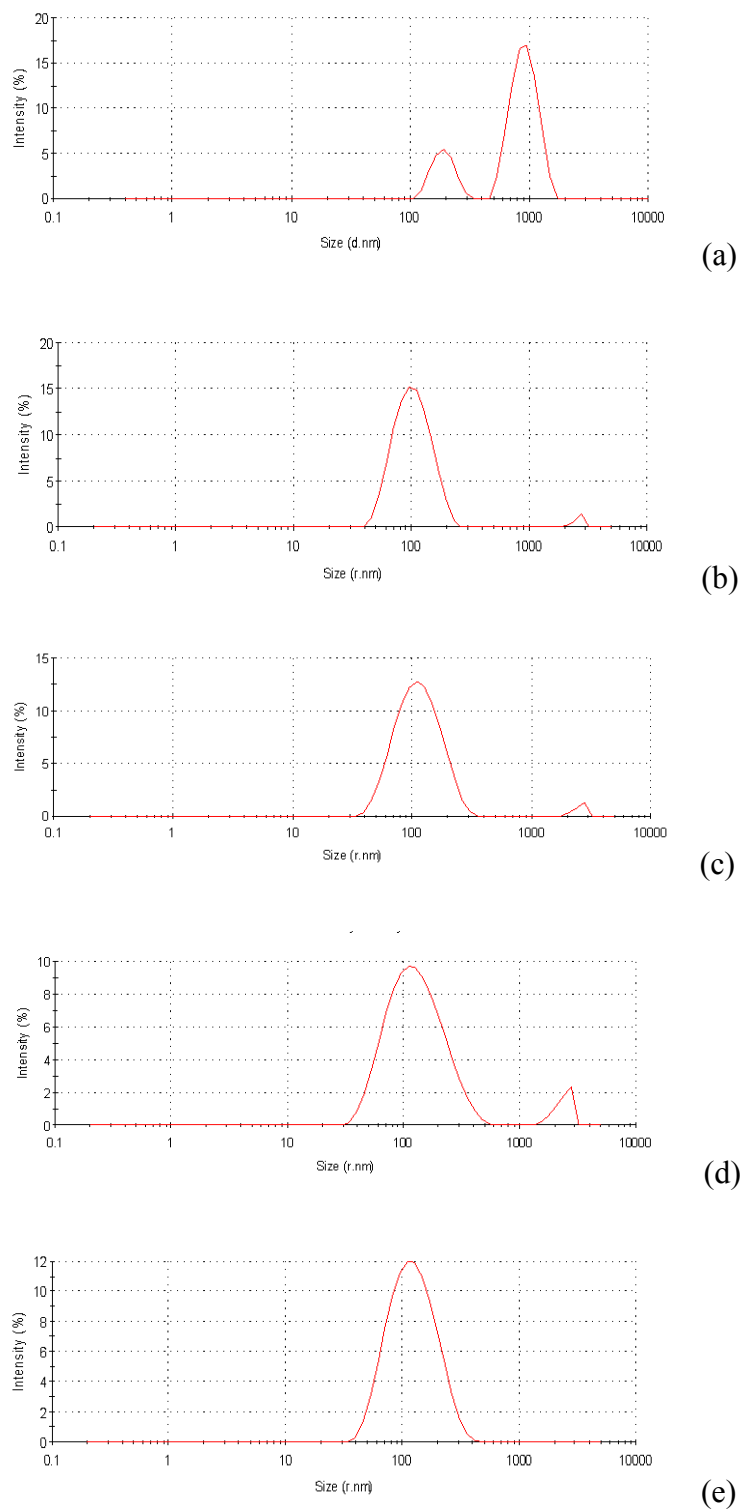


Figure 4.10 size distribution graphs of (a) non ultrasonicated sample, (b) 5 min, (c) 10 min, (d) 15 min and (e) 20 min ultrasonicated samples.

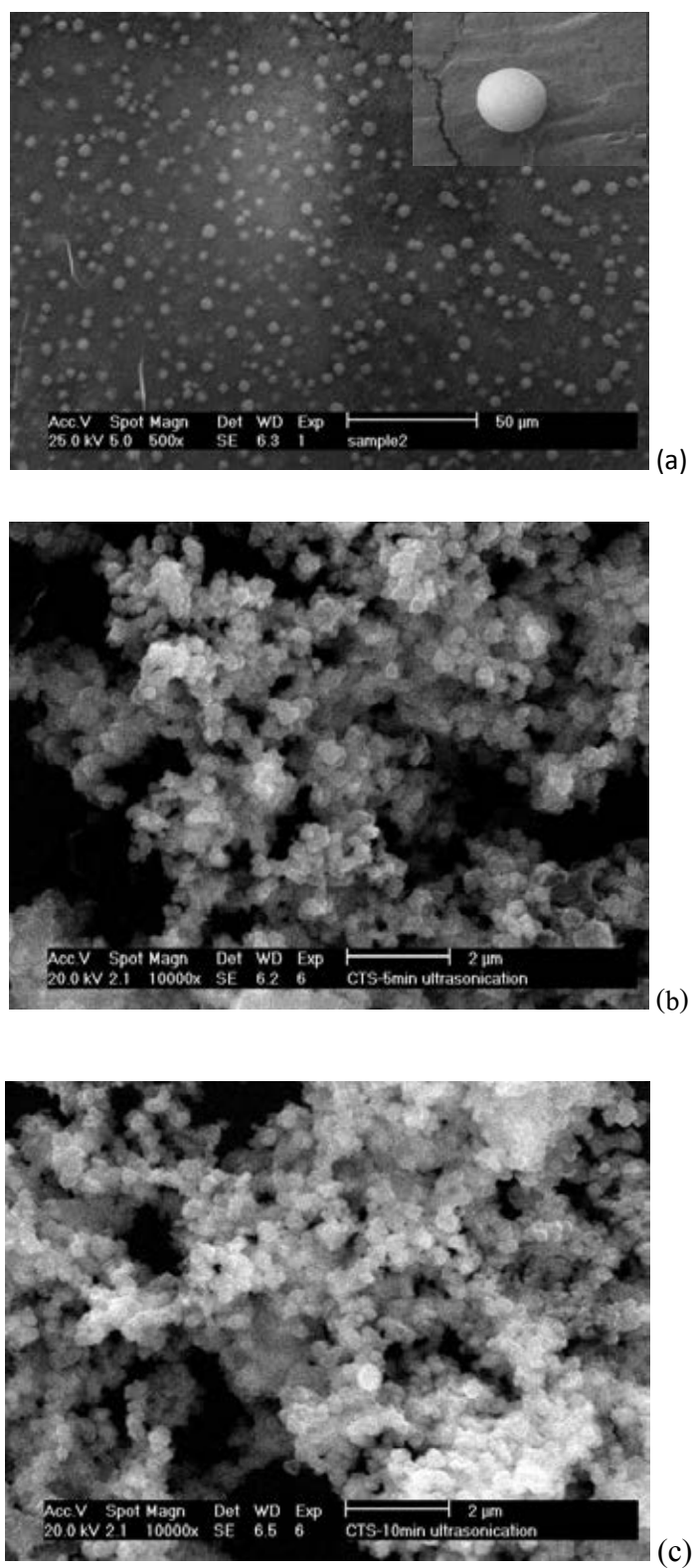


Figure 4.11 SEM images for chitosan nanoparticles of (a) non ultrasonication at wide screen and capture of one particle, (b) 5 min ultrasonication at wide screen and (d) 10 min ultrasonication at wide screen.

4.4 Preparation 5,7-DMF/HP β CD loaded chitosan nanoparticles

5,7-DMF/HP β CD inclusion complexes loaded chitosan nanoparticles (IC-CSNP) were prepared as described in section 3.3.7. Briefly, lyophilization 5,7-DMF/HP β CD inclusion complex was entrapped into the chitosan nanoparticles *via* the ionotropic gelation method and then treated by ultrasonication of 50% amplitude for 5 min.

The physicochemical properties of the ultrasonicated IC-CSNP (IC-uCSNP) with different mass ratio of inclusion complexes are shown in Table 4.5. The incorporation of amounts 5,7-DMF/HP β CD inclusion complex to the chitosan nanoparticles led to an increase in the particle size of nanoparticles.

5,7-DMF/HP β CD inclusion complex could be incorporated very efficiently to all chitosan nanoparticle formulations (Table 4.6). The entrapment efficiency decreased as increasing amount 5,7-DMF/HP β CD inclusion complex. However, this decrease in the entrapment efficiency was accompanied by increase in the loading capacity. The loading capacity in chitosan nanoparticle increased due to increased amount of inclusion complex in the formulation. The results support findings that the entrapment efficiency decreased and loading capacity increased with increasing amount of simvastatin/HP β CD into chitosan nanoparticles [42].

The incorporation of 5,7-DMF/HP β CD inclusion complex to the chitosan nanoparticles was limited at ratio of 4/4/1 and 4/8/1 w/w/w. The excess amount of loaded 5,7-DMF/HP β CD inclusion complex resulted in the decrease entrapment efficiency as compared to the ratio of 4/2/1 w/w/w. In addition, ultrasonication of IC-CSNP resulted in the increase entrapment efficiency and loading capacity. The entrapment efficiency and loading capacity of IC-uCSNP increased due to increased surface area of nanoparticle size in the ultrasonicated sample. Finally, the ratio of IC-uCSNP at 4/2/1 w/w/w was selected for *in vitro* release studies based on highest entrapment efficiency.

The morphological characteristics of IC-uCSNP at ratio of 4/2/1 and 4/4/1 w/w/w were recorded by scanning electron microscopy (SEM) and Transmission electron microscopy (TEM). SEM and TEM images (Figures 4.12 and 4.13) confirmed the spherical shape and smooth particles. The mean sizes of chitosan nanoparticle from TEM were similar to those from the particle sizer.

It was observed that the zeta potential of IC-uCSNP was higher than that of blank (without 5,7-DMF/HP β CD inclusion complex). The increasing zeta potential of IC-uCSNP may be caused by an increased free positively charged amino group of chitosan on the surface of nanoparticles due to the reduction of ionic interaction between TPP and chitosan during nanoparticles formation because of presence of 5,7-DMF/HP β CD inclusion complex molecules [55].

Table 4.5 Physicochemical properties of IC-CSNP treated by ultrasonication in the difference concentrations of 5,7-DMF/HP β CD inclusion complexes (mean \pm SD, n=3).

Ratio of CS/inclusion complex/TPP(w/w/w)	Concentration of inclusion complex (w/v)	Size (nm)	PDI	Zeta potential (mV)
4/0/1	-	195 \pm 3	0.31	+36 \pm 0.8
4/2/1	0.2	203 \pm 3	0.37	+44 \pm 0.9
4/4/1	0.4	241 \pm 10	0.36	+41 \pm 0.2
4/8/1	0.8	223 \pm 5	0.38	+41 \pm 2.1

Table 4.6 Entrapment efficiency (%EE) and loading capacity (%LC) of IC-uCSNP (mean \pm SD, n = 3)

Ratio CS/inclusion complex/TPP (w/w/w)	ultrasonication		Non ultrasonication	
	%EE	%LC	%EE	%LC
4/2/1	64.03 \pm 2.93	18.31 \pm 0.84	43.86 \pm 7.36	12.53 \pm 2.10
4/4/1	39.59 \pm 4.53	17.59 \pm 2.01	35.86 \pm 3.14	15.93 \pm 1.40
4/8/1	35.87 \pm 1.68	22.07 \pm 1.03	32.71 \pm 3.47	20.13 \pm 2.14

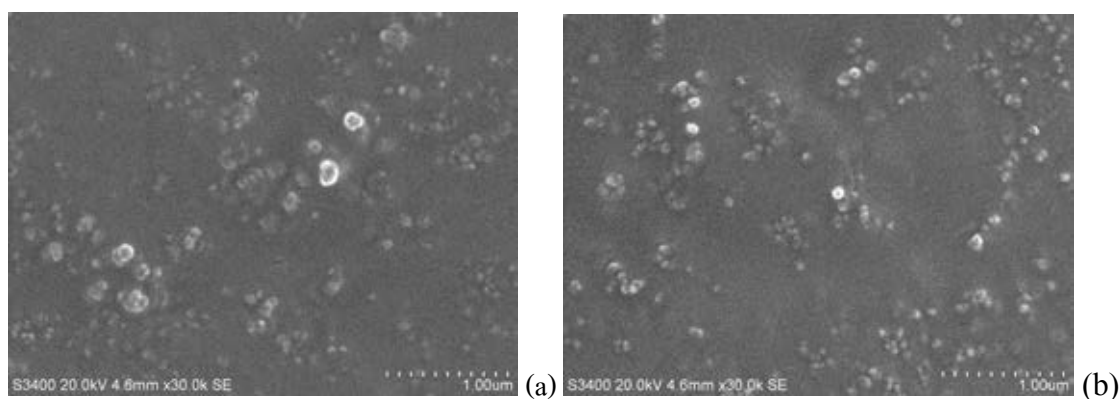


Figure 4.12 SEM images for IC-uCSNP of (a) ratio of 4/2/1 w/w/w and (b) ratio of 4/4/1 w/w/w of chitosan/inclusion complex/TPP.

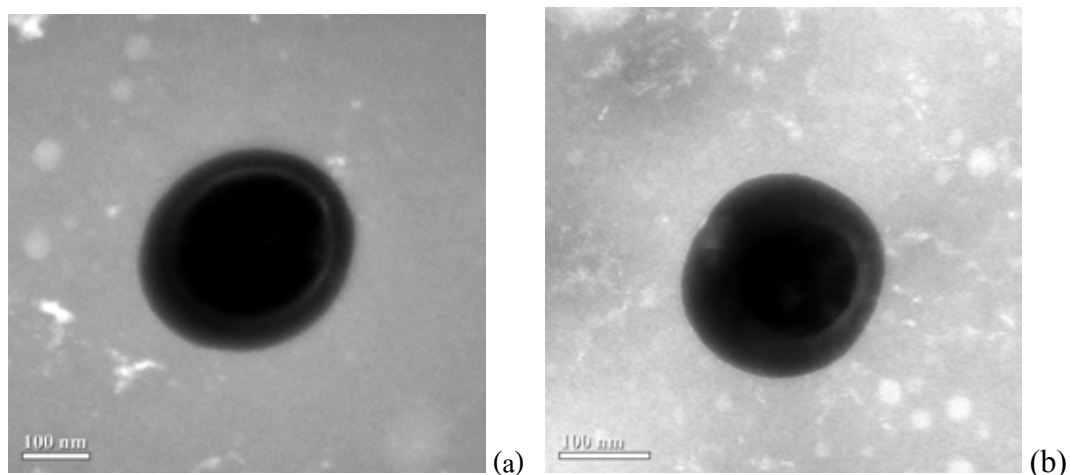


Figure 4.13 TEM images for IC-uCSNP of (a) ratio of 4/2/1 w/w/w and (b) ratio of 4/4/1 w/w/w of chitosan/inclusion complex/TPP.

4.5 *In vitro* release studies

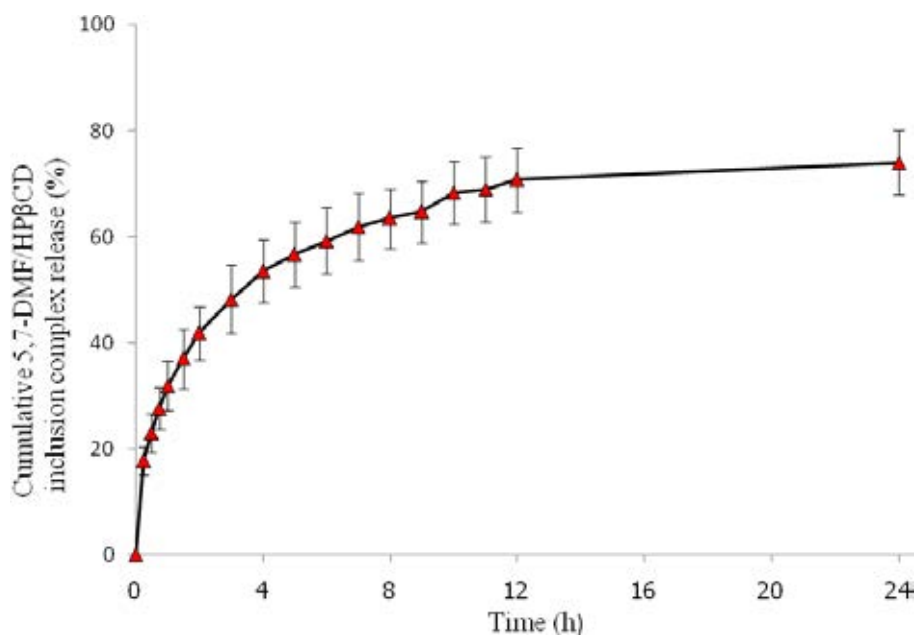
The *in vitro* release profiles of 5,7-DMF/HP β CD inclusion complex from chitosan nanoparticles in HCl (pH 1.2) and PBS (pH 7.4) are shown in Figure 4.14.

The cumulative release of 5,7-DMF/HP β CD inclusion complex from chitosan nanoparticles (IC-uCSNP ratio at 4/2/1 w/w/w) was characterized. The profile release of 5,7-DMF/HP β CD inclusion complex in HCl (pH 1.2) is shown in Figure 4.14(a). The rate of 5,7-DMF/HP β CD inclusion complex release from nanoparticles was initially rapid (27.6% within the first 45 min), and then decreased in the release rate after several hours. This indicates that the part of 5,7-DMF/HP β CD inclusion complex was adsorbed onto the nanoparticles surface, and then diffused rapidly (burst effect) when the nanoparticles came into contact with release medium. Later, inclusion complex was released slowly due to swelling or polymer degradation.

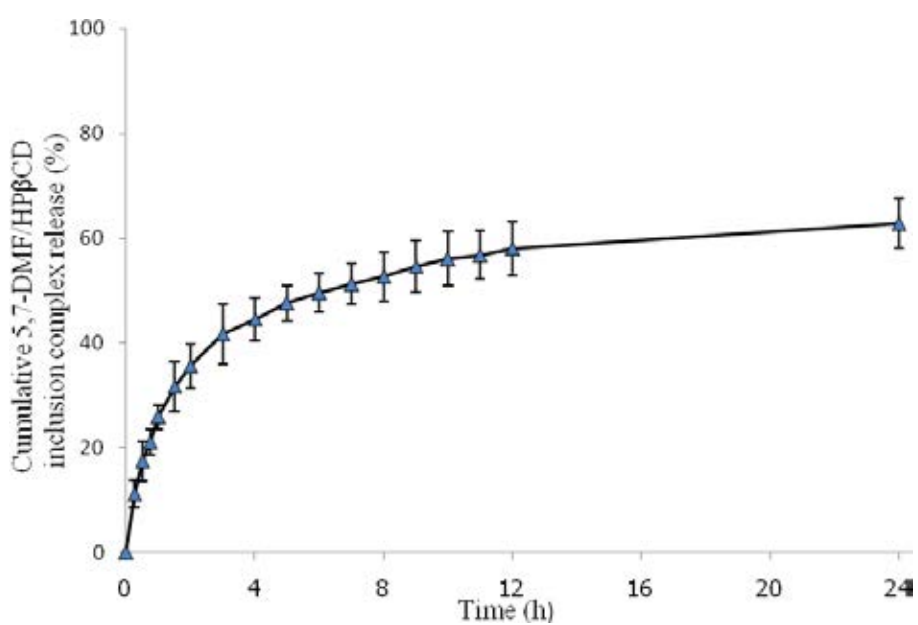
In the pH 1.2, 5,7-DMF/HP β CD inclusion complex was fast released from chitosan nanoparticles, and the released amount of 5,7-DMF/HP β CD inclusion complex was relatively high as compared to the release at pH 7.4. The higher release of inclusion complex in pH 1.2 may be explained by the swelling and dissolution of

chitosan nanoparticles caused by ionic repulsion of protonated free amino groups on chain of chitosan. Moreover, the nanoparticles of chitosan dispersed and swelled in pH 1.2. The surface area of chitosan nanoparticles in contact with the release medium may increase the release of 5,7-DMF/HP β CD inclusion complex. In contrast, the chitosan nanoparticles aggregated in PBS with pH 7.4, which may cause to reduce of the surface area of chitosan nanoparticles. The reduction surface area in contact with the release medium may reduce the release of 5,7-DMF/HP β CD inclusion complex. Additionally, the aggregation of chitosan nanoparticles in PBS can be elucidated by deprotonation of free amino groups on chains of chitosan [44].

Finally, IC-uCSNP showed the highest percent of 5,7-DMF/HP β CD inclusion complex release in pH 1.2 (simulated gastric). The result suggested that IC-uCSNP could be suitable to release the poorly soluble 5,7-DMF following oral administration and may be potentially for application as novel medicines or health promoting products.



(a)



(b)

Figure 4.14 *In vitro* release profile of 5,7DMF/HP β CD inclusion complex from chitosan nanoparticles at (a) pH 1.2 and (b) pH 7.4, 37 ± 0.1 °C (average \pm SD, n = 3).

CHAPTER V

CONCLUSION

A major flavonoid namely 5,7-dimethoxyflavone (5,7-DMF) from the rhizomes of *Kaempferia parviflora* is considerable attractive because it has many pharmacological properties. However, the pharmaceutical uses of this compound were limited due to its low water solubility. This study improved the water solubility of 5,7-DMF by preparing inclusion complexation of 5,7-DMF in HP β CD by lyophilizing method and a 1:1 stoichiometry was performed by the continuous variation (Job's plot) method. Taken the results together obtained from phase solubility, FTIR, DSC, XRD, 1D, and 2D NMR spectroscopic analysis studies suggest the formation of 5,7-DMF/HP β CD inclusion complex both in aqueous solution and in solid state. In addition, the studies have indicated that the water solubility of 5,7-DMF was greatly enhanced when the inclusion complex formed.

The water solubility of 5,7-DMF by inclusion complexation with HP β CD has been successfully improved. However, one disadvantage of cyclodextrins is its low adsorbed from gastrointestinal tract for oral administration. In spite of the water solubility improvement properties for poorly soluble compounds, its use in clinical field is limited. So inclusion complex encapsulated chitosan nanoparticles may be a promising system for enhancing absorption from gastrointestinal tract. The nanoparticles encapsulating inclusion complex can be successfully prepared by ionic cross-linking of chitosan with tripolyphosphate and resulting nanoparticles were treated by ultrasonication method. The results showed that ultrasonication decreased the mean particle size and polydispersity of nanoparticles. Chitosan nanoparticles containing 5,7-DMF/HP β CD inclusion complex have shown an high entrapment efficiency (> 60%) with average size of 203 ± 3 nm and displayed controlled release properties by an initial fast release (burst effect) followed by a slow release phase. Moreover, these results render the designed nanocarrier as possible candidates for enhancing the absorption of poorly soluble flavonoids following oral administration.

5,7-DMF/HP β CD inclusion complex loaded chitosan nanoparticle may be potentially useful for application as novel medicines or health promoting products.

REFERENCES

- [1] Rujjanawate, C., Kanjanapothi, D., Amornlerdpison, D. and Pojanagaroon, S. Anti-gastric ulcer effect of *Kaempferia parviflora*. Journal of Ethnopharmacology. 102 (2005): 120–122.
- [2] Yenjai, C., Prasanphen, K., Daodee, S., Wongpanich, V. and Kittakoop, P. Bioactive flavonoids from *Kaempferia parviflora*. Fitoterapia. 75 (2004): 89–92.
- [3] Sawasdee, P., Sabphon, C., Sitthiwongwanit, D. and Kokpol, U. Anticholinesterase activity of 7-methoxyflavone isolated *Kaempferia parviflora*. Phytotherapy Research. 23 (2009): 1792–1794.
- [4] Tep-areenan, P., Sawasdee, P. and Randall, M. Possible mechanisms of vasorelaxation for 5,7-dimethoxyflavone from *Kaempferia parviflora* in the rat aorta. Phytotherapy Research. 24 (2010): 1520–1525.
- [5] Tassaneeyakul, W. A study of anti-inflammatory activity of 5,7-dimethoxyflavone, isolated from *Boesenbergia pandurata*, in albino rats. Master's thesis, Pharmacology Faculty of Science Chiang mai University. Thailand, 1984.
- [6] Tsuji, P. A., Winn, R. N. and Walle, T. Accumulation and metabolism of the anticancer flavonoid 5,7-dimethoxyflavone compared to its unmethylated analog chrysin in the Atlantic killifish. Chemico-Biological Interactions. 164 (2006): 85–92.
- [7] Brewster, M. E. and Loftsson, T. Cyclodextrins as pharmaceutical solubilizers. Advanced Drug Delivery Reviews. 59 (2007): 645–666.
- [8] Gould, S. and Scott, R. C. 2-Hydroxypropyl- β -cyclodextrin (HP- β -CD): A toxicity review. Food and Chemical Toxicology. 43 (2005): 1451–1459.
- [9] Rinaudo, M. Chitin and chitosan: Properties and applications. Progress in Polymer Science. 31 (2006): 603–632.

- [10] Mahmoud, A. A., El-Feky, G. S., Kamel, R. and Awad, G. E. A. Chitosan/sulfobutylether- β -cyclodextrin nanoparticles as a potential approach for ocular drug delivery. International Journal of pharmaceutics. 413 (2011): 229–236.
- [11] Boonsong, S. Kra-Chai-Dam wine. Technology Chao Ban. 285 (2002) 42–43.
- [12] Tewtrakul, S., Subhadhirasakul, S., Karalai, C., Ponglimanont, C. and Cheenpracha, S. Anti-inflammatory effect of compound from *Kaempferia parviflora* and *Boesenbergia pandurata*. Food Chemistry. 115 (2009): 534–538.
- [13] Tewtrakul, S., Subhadhirasakul, S. and Kummee S. Anti-allergic activity of compounds from *Kaempferia parviflora*. Journal of Ethnopharmacology. 116 (2008): 191–193.
- [14] Wattanapitayakul, S., Chularojmontri, L., Herunsalee, A., Chansuvanich, N. and Charuchongkolwongse, S. Vasorelaxation and antispasmodic effects of *Kaempferia parviflora* ethanolic extract in isolated rat organ studies. Fitoterapia 79 (2008): 214–216.
- [15] Rujjanawate, C., Kanjanapothi, D., Amornlerdpison, D. and Pojanagaroon, S. Anti-gastric ulcer effect of *Kaempferia parviflora*. Journal of Ethnopharmacology. 102 (2005): 120–122.
- [16] Wattanapitayakul, S. K., Suwatronnakorn. M., Chularojmontri, L., Herunsalee, A., Niumsakul, S., Charuchongkolwongse, S. and Chansuvanich, N. *Kaempferia parviflora* ethanolic extract promoted nitric oxide production in human umbilical vein endothelial cells. Journal of Ethnopharmacology. 110 (2007): 559–562.
- [17] Astray, C., Gonzalez-Barreiro, C., Mejuto, J. C., Rial-Otero, R. and Simal-Gandara, J. A review on the use of cyclodextrins in foods. Food Hydrocolloids. 23 (2009): 1631–1640.
- [18] Loftsson, T. and Duchene, D. Cyclodextrins and their pharmaceutical applications. International Journal of Pharmaceutics. 329 (2007): 1–11.
- [19] Loftsson, T., Jarho, P., Masson, M. and Jarvinen, T. Cyclodextrin in drug delivery. Expert Opinion on Drug Delivery. 2 (2005): 335–351.

- [20] Del Valle, E. M. M. Cyclodextrins and their uses: A review. Process Biochemistry. 39 (2004): 1033–1046.
- [21] Higuchi, T. and Connors, K. Advances in Analytical Chemistry and Instrumentation. 4 (1965): 117–212.
- [22] Blanco, J., Vila-Jalo, J. L., Otero, F. and Anguiano S. Influence of method of preparation on inclusion complexes of naproxen with different cyclodextrins. Drug Development and Industrial Pharmacy. 17 (1991): 943–957.
- [23] Zhang, M., Li, J., Zhang, L. and Chao, J. Preparation and spectral investigation of inclusion complex of caffeic acid and hydroxypropyl- β -cyclodextrin. Spectrochimica Acta Part A: Molecular and Biomolecular Spectroscopy. 71 (2009): 1891–1895.
- [24] Yang, B., Lin, L., Chen, Y. and Liu, Y. Artemether/hydroxypropyl- β -cyclodextrin: Phase solubility and inclusion mode. Bioorganic & Medicinal Chemistry. 17 (2009): 6311–6317.
- [25] Ortega Lyng, S. M., Passos, M. and Fontana, J. D. Bixin and α -cyclodextrin inclusion complex and stability tests. Process Biochemistry. 40 (2005): 865–872.
- [26] Ficarra, R., Tommasini, S., Raneri, D., Calobro, M. L., Di Bella, M. R., Rustichelli, C., Gamberini, M. C. and Ficarra, P. Study of flavonoids/ β -cyclodextrins inclusion complexes by NMR, FTIR, DSC, X-ray investigation. Journal of Pharmaceutical and Biomedical Analysis. 29 (2002): 1005–1014.
- [27] Rezende, B. A., Cortes, S. F., De Sousa, F. B., Lula, I. S., Schmitt, M., Sinisterra, R. D. and Lemos, V. S. Complexation with β -cyclodextrin confers oral activity on the flavonoid dioclein. International Journal of Pharmaceutics. 367 (2009): 133–139.
- [28] Chen, W., Yang, L. J., Ma, S. X., Yang, X. D., Fan, B. M. and Lin, J. ClassicaulineA/ β -cyclodextrin host-guest system: preparation, characterization, inclusion mode, solubilization and stability. Carbohydrate Polymers. 84 (2011): 1321–1328.

- [29] Mesplet, N., Morin, P. and Ribet, J. P. Spectrofluorimetric study of eflucimibe- γ -cyclodextrin inclusion complex. European Journal of Pharmaceutics and Biopharmaceutics. 59 (2005): 523–526.
- [30] Liu, J., Qui, L., Gao, J. and Jin, Y. Preparation, characterization and in vivo evaluation of formation of baicalein with hydroxypropyl- β -cyclodextrin. International Journal of Pharmaceutics. 312 (2006): 137–143.
- [31] Jullian, C. Improvement of galangin solubility using native and derivative cyclodextrin: An UV-Vis and NMR study. Journal of the Chilean Chemical Society. 54 (2009): 201–203.
- [32] Misiuk, W. and Zalewska, M. Investigation of inclusion complex of tradazone hydrochloride with hydroxypropyl- β -cyclodextrin. Carbohydrate Polymers. 77 (2009): 482–488.
- [33] Wen, J., Liu, B., Yuan, E., Ma, Y. and Zhu, Y. Preparation and physicochemical properties of the complex of naragin with hydroxypropyl- β -cyclodextrin. Molecules. 15 (2010): 4401–4407.
- [34] Wu, H., Liang, H., Yuan, Q., Wang, T. and Yan, X. Preparation and stability investigation of inclusion complex of sulforaphane and hydroxypropyl- β -cyclodextrin. Carbohydrate Polymers. 82 (2010): 613–617.
- [35] Yang, L. J., Chen, W., Ma, S. X., Gao, Y. T., Huang, R., Yan, S. J. and Lin, J. Host-guest system of taxifolin and native cyclodextrin or its derivative: preparation, characterization, inclusion mode, and solubilization. Carbohydrate Polymers. 85 (2011): 629–637.
- [36] Wang, J., Cao, Y., Sun, B. and Wang, C. Characterisation of inclusion complex of trans ferulic acid and hydroxypropyl- β -cyclodextrin. Food Chemistry. 124 (2011): 1069–1075.
- [37] Eid, E. E. M., Abdul, A. M., Suliman, F. E., Sukari, M. A., Rasedee, A. and Fatah, S. S. Characterization of inclusion complex of zerumbone with hydroxypropyl- β -cyclodextrin. Carbohydrate Polymers. 83 (2011): 1707–1714.
- [38] Zhang, X., Wu, Z., Gao, X., Shu, S., Zhang, H., Wang, Z. and Li, C. Chitosan bearing pendent cyclodextrin as a carrier for controlled protein release. Carbohydrate Polymers. 77 (2009): 394–401.

- [39] Grenha, A., Seijo, B. and Remunan-Lopez, C. Microencapsulated chitosan nanoparticles for lung protein delivery. European Journal of Pharmaceutical Sciences. 25 (2005): 427–437.
- [40] Maestrelli, F., Garcia-Fuentes, M., Mura, P. and Alonso, M. J. A new drug nanocarrier consisting of chitosan and hydroxypropylcyclodextrin. European Journal of Pharmaceutics and Biopharmaceutics. 63 (2006): 79–86.
- [41] Trapani, A., Lopodota, A., Franco, M., Cioffi, N., Ieva, E., Garcia-Fuentes, M. and Alonso, M. J. A comparative study of chitosan and chitosan/cyclodextrin nanoparticles as potential carrier for the oral delivery of small peptides. European Journal of Pharmaceutics and Biopharmaceutics. 75 (2010): 26–32.
- [42] Vyas, A., Saraf, S. and Saraf, S. Encapsulation of cyclodextrin complexed simvastatin in chitosan nanocarrier: A novel technique for oral delivery. Journal of Inclusion Phenomena Macroscopic Chemistry. 66 (2010): 251–259.
- [43] Jingou, J., Shilei, H., Weiqi, L., Danjun, W., Tengfei, W. and Yi, X. Preparation, characterization of hydrophilic and hydrophobic drug in combine loaded chitosan/cyclodextrin nanoparticles and *in vitro* release study. Colloids and Surfaces B: Biointerfaces. 83 (2011): 103–107.
- [44] Keawchaon, L. and Yoksan, R. Preparation, characterization and *in vitro* release study of carvacrol-loaded chitosan nanoparticle. Colloids and Surfaces B: Biointerfaces. 48 (2011): 163–171.
- [45] Santos, H. M., Lodeiro, C. and Capelo-Martinez, J. L. The power of ultrasound. In J. L. Capelo-Martinez (ed.), Ultrasound in Chemistry: Analytical Applications, pp. 1–16. Weinheim: Wiley-VCH, 2009.
- [46] Chen, R. H., Chang, J. R. and Shyr, J. S. Effect of ultrasonic conditions and storage in acedic solutions on changes in molecular weight and polydispersity of treated chitosan. Carbohydrate Research. 299 (1997): 287–294.

- [47] Tang, E. S. K., Huang, M. and Lim, L. Y. Ultrasonication of chitosan and chitosan nanoparticles. International Journal of Pharmaceutics. 265 (2003): 103–114.
- [48] Tsai, M. L., Bai, S. W. and Chen, R. H. Cavitation effect versus stretch effects resulted in different size and polydispersity of ionotropic gelation chitosan-sodium tripolyphosphate nanoparticles. Carbohydrate Polymers. 71 (2008): 448–457.
- [49] Edlund, U. and Albertsson, A. C. Degradable polymer microspheres for controlled drug delivery. Advances in polymer science. 157 (2002): 68-91.
- [50] Agnihotry, S. A., Mallikarjuna, N. N. and Aminabhavi, T. M. Recent advances on chitosan-based micro- and nanoparticle in drug delivery. Journal of Controlled Release. 100 (2004): 5–28.
- [51] Krauland, A. H. and Alonso, M. J. Preparation Chitosan/cyclodextrin nanoparticles as macromolecular drug delivery system. International Journal of Pharmaceutics. 340 (2007): 134–142.
- [52] Ammar, H. O., El-Nahhas, S. A., Ghorab, M. M. and Salama, A. H. Chitosan/cyclodextrin nanoparticles as drug delivery system. Journal of Inclusion Phenomena Macrocyclic Chemistry. 44 (2009): 320–325.
- [53] Job, P. Formation and stability of inorganic complexes in solution. Annali Di Chimica Applicata. 9 (1928). 113–203.
- [54] Zhu, L., Huo, Z., Wang, L., Tong, X., Xiao, Y. and Ni, K. Targeted delivery of methotrexate to skeletal muscular tissue by thermosensitive magnetoliposomes. International Journal of Pharmaceutics. 370 (2009): 136–143.
- [55] Trapani, A., Garcia-Fuentes, M. and Alonso, M. J. Novel drug nanocarriers combining hydrophilic cyclodextrins and chitosan. Nanotechnology. 19 (2008): 1–10.

APPENDICES

Appendix A

Absorption spectra of 5,7-DMF, HP β CD and their inclusion complex

In part I, the amount of free 5,7-DMF could be obtained from directly measuring the absorption of inclusion complex in DI water and then determined the amount of 5,7-DMF from a calibration curve of free 5,7-DMF in ethanol (Figure B1). To prove this, we did the experiments A1 and A2 to confirm that, at λ 264 nm, 5,7-DMF in ethanol and 5,7-DMF/HP β CD complex in DI water gave the same absorption intensity and no absorption of free HP β CD interfered the results. Moreover, no shiftment of maximum absorption peaks between 5,7-DMF in ethanol and 5,7-DMF/HP β CD complex in DI water was observed.

In part II, the amount of free 5,7-DMF in 5,7-DMF/HP β CD complex was evaluated before starting the experiment using the method described above. This data are necessary for calculating the amount of inclusion complex in the medium as following described. In the releasing experiment, the absorption of medium was measuring and use this value for determining the amount of free 5,7-DMF by using the calibration curve of free 5,7-DMF in ethanol. Then comparing this amount of 5,7-DMF with the starting 5,7-DMF in inclusion complex to calculate the amount of inclusion complex release. In the experiment A3, the absorptions of inclusion complex in water, ethanol and buffer were characterized to prove that the absorption intensities of inclusion complex were the same in all medium.

A1: Absorption spectra of 5,7-DMF, HP β CD and 5,7-DMF/HP β CD inclusion complex

The absorption spectra of 5,7-DMF, HP β CD and 5,7-DMF/HP β CD inclusion complex were determined by following method. Briefly, 2.8 mg of 5,7-DMF, 13.8 mg of HP β CD and an inclusion complex between 5,7-DMF (2.8 mg) and HP β CD (13.8 mg) were individually added in 10 ml of deionized water. The samples were shaken in a thermostatic shaking water bath at 37 ± 0.1 °C for 24 h and filtered using 0.45 μ m Nilon filter. The absorption spectrum of each filtrate was analyzed by the Agilent 8453 UV/Vis spectrophotometer. Deionized water was used as blank medium.

The absorption spectra of the results were showed in Figure A1. The absorption profiles of free 5,7-DMF and 5,7-DMF/HP β CD in DI water were the same. The maximum wavelengths of both samples were 264 nm. And no absorption of HP β CD was found in a range of 200-500 nm. Therefore, measurement of the absorption intensity at $\lambda = 264$ nm of inclusion complex could be used for determination the amount of 5,7-DMF in an inclusion complex.

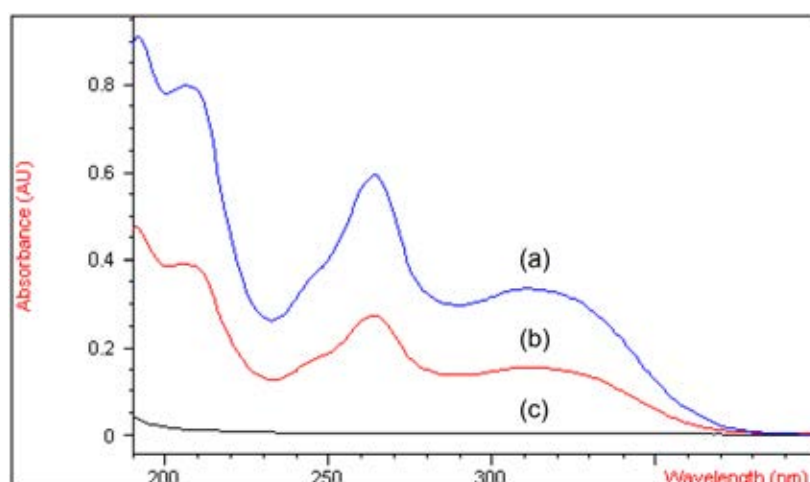


Figure A1 UV spectra of (a) 5,7-DMF in the presence of HP β CD, (b) 5,7-DMF, (c) HP β CD.

A2: The absorption intensity of free 5,7-DMF and 5,7-DMF in inclusion complex

The experiment was done by measuring the absorption intensity of five different concentration of 25 ml clear inclusion complexes solution using Agilent 8453 UV/Vis spectrophotometer. Subsequently, each solution was extracted with dichloromethane to separate 5,7-DMF from 5,7-DMF/HP β CD inclusion complex. The dichloromethane layer was removed by vacuum evaporator to obtain free 5,7-DMF. The solid 5,7-DMF was then re-dissolved in 25 ml of ethanol and analyzed the absorption intensity by UV/Vis spectrophotometer.

The results in Table A1 showed the absorption intensities of 5,7-DMF/HP β CD complex in DI water were not significantly different from those of extracted 5,7-DMF

in ethanol ($n = 2$, ANOVA, $P > 0.05$). This could be indicated that we can directly determined the amount of free 5,7-DMF in complex by measuring the absorption intensity of 5,7-DMF/HP β CD complex.

Table A1 The absorbance of 5,7-DMF in the presence of HP β CD (before extraction) in 25 ml of deionized water and the absorbance of 5,7-DMF in the absence of HP β CD (after extraction) in 25 ml of ethanol ($\lambda_{\max} = 264$ nm, $n=2$)

samples	Before extraction	After extraction
1	0.30431	0.28683
2	0.43167	0.39187
3	0.60940	0.59413
4	0.74274	0.76621
5	1.04135	1.07185

A3: The absorption intensity of 5,7-DMF/HP β CD inclusion complex in different medium

The experiment was done by dissolving 25 mg of inclusion complexes in 25 ml of each medium; deionized water, ethanol, hydrochloric acid and phosphate buffered saline. Subsequently, the samples were analyzed the absorption intensity by UV/Vis spectrophotometer.

The results were showed in Table A2 indicated that the absorption intensity of the inclusion complex in different medium were no significant difference ($n = 3$, ANOVA, $P > 0.05$).

Table A2 The absorbance of 5,7-DMF in the presence of HP β CD in the 25 ml of the difference solvents ($\lambda_{\text{max}} = 264 \text{ nm}$, $n=3$)

solvents	Absorption intensity			Mean
	n 1	n 2	n 3	
Deionized water	0.50168	0.50602	0.49121	0.49964
Ethanol	0.49175	0.50966	0.50652	0.50264
Hydrochloric acid	0.49724	0.49639	0.50867	0.50077
Phosphate buffered	0.50461	0.49522	0.49790	0.49924

Appendix B

Calibration curve for determining the amount of 5,7-DMF

The experiment was done by dissolving 10 mg of 5,7-DMF with ethanol into a 50 ml volumetric flask. This sample was used as a stock solution and was further diluted to be the concentration of 0.5 to 10 $\mu\text{g/ml}$ with ethanol in volumetric flasks. The absorbance of each solution was determined by UV/Vis spectrophotometer (Agilent 8453) at wavelength of 264 nm and ethanol was used as a blank medium.

The absorbance and a standard calibration curve of 5,7-DMF were presented in Table B1 and Figure B1, respectively. The linear relationship between concentration of 5,7-DMF and absorbance showed a coefficient of determination curve (R^2) of 0.999. This calibration curve was further used for calculating the amount of 5,7-DMF.

Table B1 The absorbance of 5,7-DMF in ethanol solution determined at 264 nm.
(n=3)

Concentration of 5,7-DMF ($\mu\text{g/ml}$)	Absorbance				
	n 1	n 2	n 3	Mean	SD
0.5	0.05090	0.05226	0.04950	0.05089	0.0014
1	0.10152	0.09731	0.09689	0.09857	0.0026
2	0.18739	0.19060	0.18428	0.18742	0.0032
3	0.27946	0.27895	0.28013	0.27951	0.0006
4	0.36695	0.37014	0.36632	0.36780	0.0020
5	0.45985	0.45971	0.46000	0.45985	0.0001
6	0.57020	0.56577	0.57102	0.56900	0.0028
7	0.66011	0.65569	0.65916	0.65832	0.0023
8	0.75493	0.75255	0.75643	0.75464	0.0020
9	0.83614	0.85584	0.83719	0.84306	0.0111
10	0.92640	0.92642	0.93159	0.92814	0.0030
11	1.01160	1.01590	1.01860	1.01537	0.0035
12	1.10220	1.10870	1.10320	1.10470	0.0035

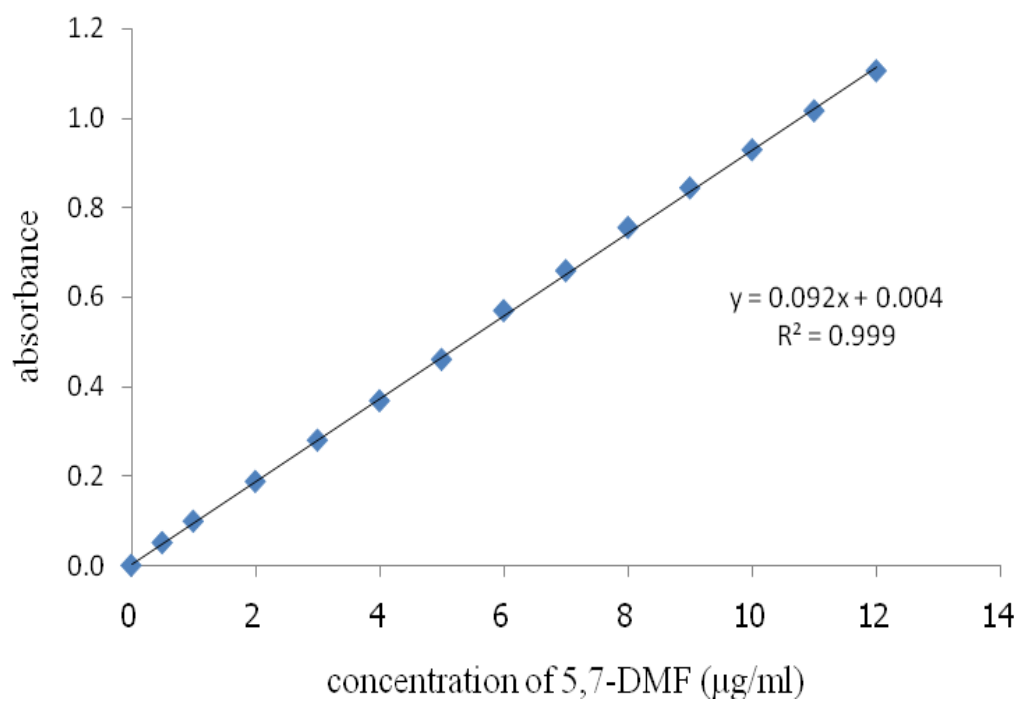


Figure B1 The standard calibration curve of 5,7-DMF in ethanol.

Appendix C

Phase solubility studies

Table C1 The Solubility data of 5,7-DMF in various HP β CD concentrations.

Conc. of HP β CD (mM)	Absorbance of 5,7-DMF (264nm)			Concentration of 5,7-DMF (mM)				
	n 1*	n 2**	n 3**	n 1	n 2	n 3	Mean	SD
0	0.18415	0.31964	0.50515	0.0069	0.0122	0.0193	0.0128	0.01
2	0.27539	0.21363	0.23288	0.0731	0.0484	0.0529	0.0582	0.01
4	0.44953	0.38097	0.40786	0.1201	0.0871	0.0933	0.1002	0.02
6	0.61938	0.59968	0.62489	0.1659	0.1376	0.1434	0.1490	0.01
8	0.83573	0.80254	0.80421	0.2242	0.1845	0.1849	0.1978	0.02
10	1.00223	1.00078	1.03703	0.2691	0.2303	0.2387	0.2460	0.02

* The samples at 2-10 mM of HP β CD were diluted 7 times.

** The samples at 2-10 mM of HP β CD were diluted 6 times.

Appendix D

Stoichiometry determination

Table D1 Absorbances of 5,7-DMF/HP β CD, pure 5,7-DMF and Δ absorbance in deionized water.

Absorbance (264 nm)			
5,7- DMF/HP β CD	5,7-DMF pure	Δ Abs.	R*
0	0	0	0
0.12941	0.11746	0.01196	0.1
0.26006	0.24048	0.01958	0.2
0.38172	0.35577	0.02595	0.3
0.51103	0.47434	0.03669	0.4
0.65449	0.57301	0.08148	0.5
0.75362	0.69670	0.05691	0.6
0.86130	0.81804	0.04326	0.7
0.95656	0.92048	0.03608	0.8
1.05217	1.03310	0.01907	0.9
0	0	0	1

*R = [5,7-DMF]/([5,7-DMF]+[HP β CD]).

Appendix E

Size distribution graphs

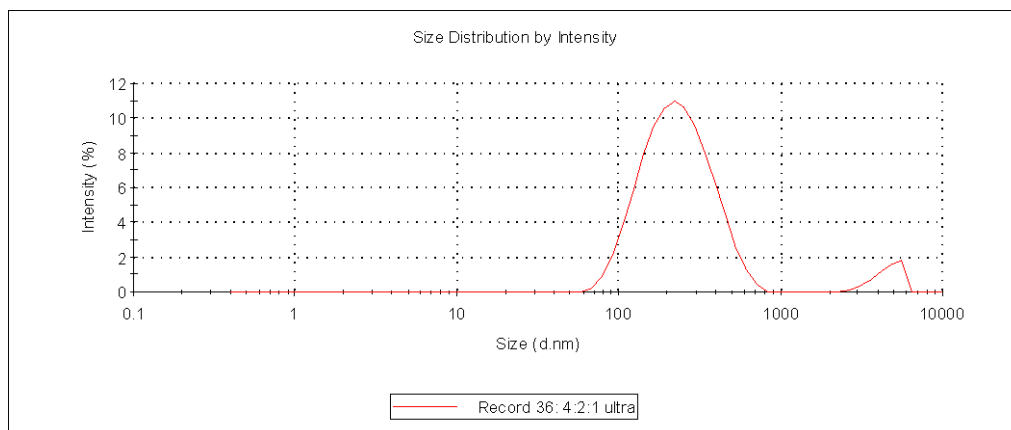


Figure E1 The size distribution graph of IC-uCSNP at ratio of chitosan/inclusion complex/TPP as 4/2/1 (w/w/w).

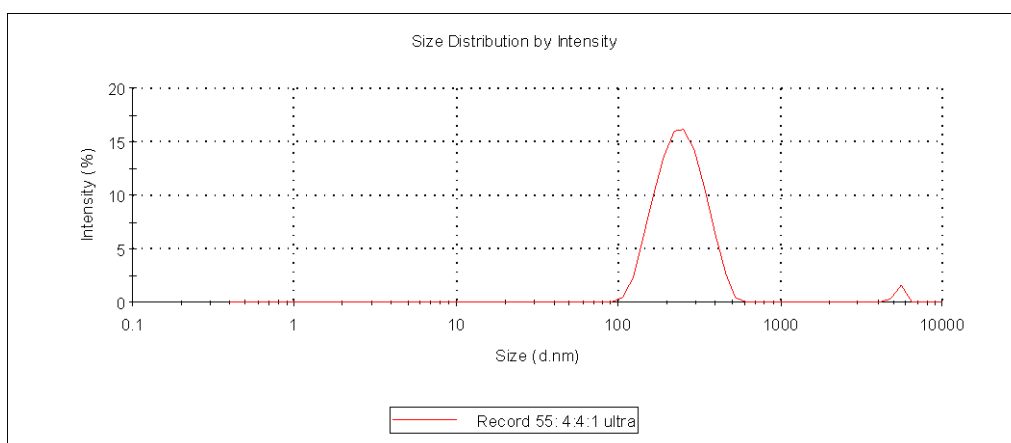


Figure E2 The size distribution graph of IC-uCSNP at ratio of chitosan/inclusion complex/TPP as 4/4/1 (w/w/w).

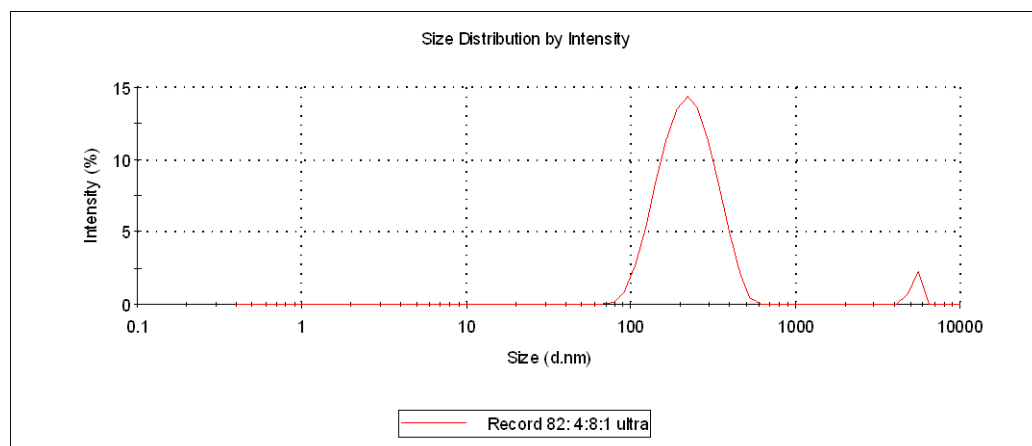


Figure E3 The size distribution graph of IC-uCSNP at ratio of chitosan/inclusion complex/TPP as 4/8/1 (w/w/w).

Appendix F

Percentage of Cumulative inclusion complex Release

Table F1 Percentage of 5,7-DMF/HP β CD inclusion complex release from chitosan nanoparticles in HCl (pH 1.2).

%5,7-DMF/HP β CD inclusion complex release from chitosan nanoparticles						
Time	1	2	3	Mean	SD	
15 min	15.9	20.7	16.5	17.7	2.6	
30 min	20.2	27.1	21.7	23.0	3.6	
45 min	24.4	32.1	26.3	27.6	4.0	
1 h	27.6	37.0	31.0	31.8	4.7	
1.30 h	32.7	43.4	35.0	37.0	5.7	
2 h	37.1	47.1	41.1	41.8	5.0	
3 h	43.3	55.5	45.8	48.2	6.4	
4 h	49.2	60.2	51.1	53.5	5.9	
5 h	51.8	63.6	54.5	56.6	6.2	
6 h	54.4	66.4	56.9	59.3	6.3	
7 h	57.3	69.2	59.4	62.0	6.4	
8 h	59.7	69.8	60.8	63.4	5.6	
9 h	60.2	71.2	62.8	64.7	5.8	
10 h	-	72.5	64.2	68.4	5.9	
11 h	-	73.3	64.6	69.0	6.1	
12 h	-	75.0	66.5	70.8	6.0	
24 h	68.3	80.5	73.3	74.0	6.1	

Table F2 Percentage of 5,7-DMF/HP β CD inclusion complex release from chitosan nanoparticles in PBS (pH 7.4).

Time	%5,7-DMF/HP β CD inclusion complex release from chitosan nanoparticles				
	1	2	3	Mean	SD
15 min	13.9	10.9	8.6	11.1	2.7
30 min	21.3	17.4	13.7	17.5	3.8
45 min	22.7	22.1	18.3	21.0	2.4
1 h	26.3	27.8	23.4	25.8	2.3
1.30 h	35.8	32.8	26.4	31.7	4.8
2 h	39.1	36.8	30.8	35.6	4.2
3 h	44.5	45.4	35.1	41.7	5.7
4 h	46.0	47.7	39.8	44.5	4.2
5 h	48.6	50.2	43.9	47.5	3.3
6 h	50.5	52.6	45.5	49.5	3.6
7 h	51.5	55.0	47.2	51.2	3.9
8 h	52.9	57.1	47.9	52.6	4.6
9 h	55.1	59.4	49.5	54.7	5.0
10 h	55.4	61.4	51.2	56.0	5.1
11 h	56.9	61.4	52.1	56.8	4.7
12 h	58.5	62.8	52.6	58.0	5.1
24 h	62.2	67.8	58.4	62.8	4.7

VITAE

Name : Mr. Supachai Songngam
Date of birth : July 9, 1986
Nationality : Thai
Address : 35, Moo 2, Kangann, Prasat, Surin, 32140
University Education : Bachelor's Degree from Department of Chemistry,
Faculty of Science, Srinakarinwirot University, 2005-
2008

Master's Degree from Program in Petrochemistry and
Polymer Science, Faculty of Science,
Chulalongkorn University, 2009-2011

Conference attendance : Poster presentation, Proceeding "Inclusion complex of
5,7-dimethoxyflavone with 2-hydroxypropyl- β -
cyclodextrin" at The 6th Pure and Apply Chemistry
International Conference 2012, The Empress
Convention Center, Chiang Mai, Thailand